Clin Schizophr Relat Psychoses
Spl 1, 2020
DOI: 10.3371/CSRP.GJ.112820

Clinical Schizophrenia & Related Psychoses

Research Article

Hybrid Open Access

Gallilean Black Hole Transformations for the Anti COVID19 RoccuffirnaTM Drug Design

Grigoriadis Ioannis

Biogenea Pharmaceuticals Ltd, Pharmaceutical Biotechnology Company, Thessaloniki, Greece

Abstract

SARS coronavirus 2 (SARS-CoV-2) encoding a D614G mutation in the viral spike (S) protein predominate over time in locales where it is found, implying that this change enhances viral transmission. It has also been observed that retroviruses pseudotyped with SG614 infected ACE2-expressing cells markedly more efficiently than those with SD614. It is thought that all of the rich content in the present-day Universe based on an array of recent observations developed through gravitational amplification of primeval density fluctuations generated in the very early phase of cosmic evolution. In this paper, we strongly combine machine learning characteristics, efficient in computing resource usage, and powerful to achieve very high accuracy levels for the in-silico generation of the RoccuffirnaTM small molecule, a less toxic nano-ligand targeted the COVID-19-D614G mutation using Quantum Kerr-(A)dS and Myers–Perry black microBlackHole-Inspired Gravitationals for both Euclidean and Lorentzian signatures in Practice. We provide also an extensive toolbox of methods for performing quantum communication, Neural Matrix Factorizations, cryptography, Schrodinger inspired docking algorithms, teleportation and other information-theoretic tasks in MathCast programming language, and compared these algorithms by means of mean percentile free energy ranking, in a new recall-based evaluation metric for the in-silico design of a Novel Series of Sivirinavir TMQMMMCoRoNNARRFr anti-(nCoV-19) annotated ligands. We finally, discuss various general results including heuristic horizon topology, and near-horizon fragmentation symmetry ranging from supergravity theories to enhance the Roccuffirna's gravity to trap the SARS-COV-2 viruses in practice.

Keywords: COVID19 •Neural Networks •Quantum Kerr-(A)Ds •Myers–Perr •Black microBlackHole-Inspire •D Gravitationals •Euclidean and Lorentzian signatures •Quantum-Inspired Evolutionary Algorithm, QSAR •Artificial intelligence •Data mining •Machine learning •Drug designing •Chemoinformatics

Introduction

The emergence of the new Severe acute respiratory syndrome coronavirus 2 (SARS-CoV-2), coronavirus (nCoV-19) has brought tremendous impact on worldwide health [1-5], whilst the chemogenomic interactions between the virus and the human is widely recognized to be critical foundation in responding the current outbreak the of the COVID2019 disease [6-12]. The virus was initially detected in Himalayan palm civets (Guan et al., 2003) that may have served as an amplification host; the civet virus contained a 29-nucleotide sequence not found in most human isolates that were related to the global epidemic [1-4,13-16] It has been speculated that the function of the affected open reading frame (ORF 10) might have played an important role in the trans-species jump infections [17-21]. A similar virus was found later in horseshoe bat [13-25]. Structural and biochemical characterizations have indicated to us that a 29-bp insertion in ORF 8 of bat-SARS-CoV genome, not found in most human SARS-CoV genomes, was suggestive of a common ancestor with civet SARS-CoV [11-27]. Equilibrium black-hole solutions to Einstein's equations have been known since the advent of general relativity. By studying quantum fields in a black-hole background, Hawking demonstrated that this is not a mere analogy and in fact quantum mechanically black holes are a thermodynamic system. Tools for artificial intelligence and data mining can derive in an objective and reproducible manner (Quantitative) Structure-Activity Relationships ((Q)SARs) for toxicity. In this article, we discuss the various ways whereas extremal black hole near-horizon geometries in modern studies of quantum gravity applied in an alternative topological quantum computing optimization framework for the computation of topological invariants of knots, links and tangles through a stochastic discrete optimization procedure to rule out possible black-hole horizon topologies, in diverse dimensions and theories. We also investigated very specific problems with idealized 2D chemical symmetries to simplifying free energy assumptions regarding the entropy behavior, and the interactions among the protein-ligand complexes [28-30]. Our technique is motivated by a Bayesian approach to quantum mechanics, and relies on the noiseless subsystem method of quantum information science whereas Einstein's chaotic as well Mixmaster behaviors can be studied in the context of Hamiltonian dynamics, with the Hamiltonian 2H=−p2Ω+p2++p2−+e4Ω(V−1), to protect quantum states against undesired noise. The relational theory naturally predicts a fundamental decoherence mechanism, so an arrow of time emerges from a time-symmetric theory. Moreover, our model circumvents the problem of the "collapse of the wave packet" as the probability interpretation is only ever applied to diagonal density operators [30-34]. Here we investigated the conditions under which, in quantum theory, an account in terms of absolute quantities can provide a good approximation of relative quantities and topological descriptors for finding eigenvectors and eigenvalues of the combinatorial Lamerckian-Laplacian paired with advanced machine learning algorithms, such as the data mining and machine learning techniques with the AI-Quantum computing, entanglement complexity guidelines for (Q)SAR requirements as well as performance implications, random forest (RF), deep neural network (DNN), and gradient boosting decision tree (GBDT), to facilitate their applications to quantitative toxicity and fragment based drug design predictions [34-37]. In this hybrid drug designing approach, we have merged pharmacophoric elements into the RoccuffirnaTM mergednano-structures as a system of intrinsically positioned cables filtered before evaluation and triangular bars kinematically stable to the present; [35-39] from the purely geometrical dynamics of the initial singularity and structurally valid

***Corresponding Author:** John-Ioannis Grigoriadis, Grigoriadis Ioannis Pharmacist, Biogenea Pharmaceuticals Ltd, Pharmaceutical Biotechnology Company, Thessaloniki, Greece, Tel: +30 2310 282835; E-mail: biogeneadrug@gmail.com*

Received 23 September, 2020; **Accepted** 05 October, 2020; **Published** 13 October, 2020

symmetric formations of connected small molecule components, holes, [40-42] and voids jointed at their ends by hinged connections to form a rigid chemical scaffold with anti-COVID19 properties [1,4-22,23-43].

Materials and Methods

Public Datasets, SARS-COV-2 motif peptide consensus strategy.

For the N protein, we clustered 31 conformations [10,13-24,27] from the 1731 full-length SARS-CoV-2 sequences with Glu174 present in an opened conformation out of a total of 40 states present in the NMR-derived structure (PDB codes, 6xs6,1xak,6lu7) [1-11,14,15-29,34] to select a small subset representative of the protein flexibility downloaded from NCBI (30 April 2020, txid2697049, minimum length = 29,000 bp) and aligned using MAFFT [2-9,15,19]. The alignment was visually inspected and curated using Genbank NC_045512.2 as a coordinate reference suggestive of RSFIEDLLFNKV, e.g. KNFIDLLLAGF in genomes such as the ball python genome, between the Wuhan isolate beyond the limit of serious detection and spike protein nidovirus 1 of the reptile shingle back by using NC_045512.2 annotated Open Reading Frames (ORFs) plus additional ORFs.

Screening library and COVID2019 targets.

Virtual screening and Highthroughput docking molecular docking were implemented to a collection of 9591 drugs including 2037 chemicla structures of FDA-approved small molecule drugs and over 6000 herbals and phytical exctracts from the NuBBEDB updated database to uncover chemical and biological information from Brazilian biodiversity [5,6-10,14]. Drugs having a number of non-hydrogen atoms below 5 or above 100, drugs having MW > 1200, and drugs that incorporate elements not associated with organic molecules (e.g., Hg, Pt, Fe, etc.) were not considered. Note that this number is higher than the original due to the enumeration of drugs into enantiomer, tautomer, and protomer alternatives [7,8,11-14]. Virtual screening which is a technique largely based on its libraries of small molecules and the target sites was implemented using standard Web technologies such as HTML, CSS and JavaScript (AJAX) including text-based, graphics and spectral files [9,13-14]. Protein-molecule complexes, while the server itself is implemented using Java/Servlets with Hibernate, an object-relational mapping database framework followed by structural relaxation were generated through flexible-ligand:rigid-receptor molecular docking in this local energy minimization to optimize protein-molecule interactions capping the N- and C-terminal of each fragment with i-GEMDOCK and DOCK-6 through cycles in amino-acids within 4 Å of any docked molecule as considered free of local energy minimization [14,15-21]. When more than one form of the screened drug (e.g., more than one enantiomer, more than one protomer, etc.) was screened, only the form having the highest GP value was considered in the final ranking [14,16,29]. Finally, drugs were ranked according to descending GP values.

Pharmacophoric-ODEs fragmentating, merging and recoring of the selected Hit compounds: Biogenetoligandorol AI-microBlackHole heuristic algorithm

The patterns of this Biogenetoligandorol fragmentation scheme are sorted into the workings of the Galilean transformation by examining the “extended” Galilean transformation based on a set of heuristically determined descriptors to a rigid system having an arbitrary time-dependent acceleration. These descriptors can be, for example, the number of atoms describing the pattern and be determined by the substitution ip of the Galilean Transformation in Quantum Mechanics(22) while in S':/ « L jj’d, i ”L\^d,tys' = e 2h" <p, + e2*<’ (p2= eAm = m\- m2.(V\ + eAm ; ^2d/2* ° <P2),v = dx = dH dp = Dh dt dp dt dx (43-57) (r, t) = eiJ{r,t) (p(r', t). V'ip = (V'ip + iV 'f) eif, V'2ip = {V'2ip + 2iV'f-V'(p+(pV'2f+ <p(V'f)2)e‘f,i>= (f)+ if<p) eif,and the Schrödinger equation becomes n 2 2 m (V,z(p + 2 iV'f-V'(p+ i(pV f - (V 'fY <p)= ifi [(<p + if(p) -g.(V '(p + i(pv' f)] where p+2 are the the number of bonds available or the number of double bonds. The complete fragmentation scheme is analyzed to find patterns that are contained within the selected 10 hit compounds of the Colchicine, Ritonavir, Favipinavir, Balanitin, Baueronol, Chlorogenin, Behenic acid, Aristolochic acid, Asparagusate, Aspartic acid chemical structures. Whenever searching for a specific pattern, if the group has such a parent pattern, the parent pattern is searched first eliminate the terms in V'(p,which gives f = — %-r'+ g(t). One can eliminate the unwanted Vip term by the substitution ip(r, t) = eiJ{r,t) (p(r', t). (43-47) Then, V'ip = (V'ip + iV 'f) eif,V'2ip = {V'2ip + 2iV'f-V'(p+(pV'2f+ <p(V'f)2)e‘f, i>= (f)+ if<p) eif, and the Schrödinger equation becomesn 2 (43-48) 2 m(V,z(p + 2 iV'f-V'(p+ i(pV f - (V 'fY <p)= ifi [(<p + if(p) -g.(V '(p + i(pv' f)]. (43-49) One can choose/such as to eliminate the terms in V'(p, which gives f = — %-r'+ g(t). Then one can choose n g{t) such as to eliminate the purely time-dependent terms, which by definition is the near-horizon geometry, must also satisfy the Einstein equations.and one finally arrives at, = * (2mV '2(p + mf; r'(p = ih(p,ipir, t) =— ea h J (pir',t). (34-42) of the strong equivalence principle in quantum theory. After that, the solutions near the near-horizon limit of the energy momentum tensor singularity are described qualitatively by a discrete map [10,11] to verify that the ab and +– components of the Einstein equations representing different sequences of Kasner spacetimes ds2 = –dt2 + t2p1dx2 + t2p2dy2 + t2p3dz2,
for the near-horizon geometry give the following equations on the cross section H with time changing exponents pi, but otherwise constrained by p1+p2+p3=p21+p22+p23=1 whereas the child pharmacophoric pattern is searched in an inertial repeated merged system S asip = % (ml5 r, t) + ip2im2, r, t). (21-42) must imply the spacetime conservation equation μTμ = 0. Here, e is the internal energy of the particle M. Non-relativistically, the mass and enery of the particle of the energy momentum tensor , a in terms of T+–, Tab are conserved separately. Relativistically, M = 2 my, y= (1 - v2/c2)~112, (2 a, b, c) M = 2 m + etc2. There is no conflict here since relativistically, M = 2m + 0(v2/c2). (43-44) Then assume that one fragmented pharrmacophore can describe the same superposition in an accelerating to a larger ligand-receptor system S' that obeys (14), with § = £(r), £(0) = £(7) = 0, ++ and +a components of the Einstein equations are S++ = and S+a = a respectively, so that the system S' performs a conserved angular momentum associated with a rotational symmetry closed quantum circuit and coincides with the chemical structure system the S at times t = 0 and t=T, such that r ’ iT) = r(7). (25-34,37) To avoid incomplete group assignments, whenever a part of the selected 10 Colchicine, Ritonavir, Favipinavir, Balanitin, Baueronol, Chlorogenin, Behenic acid, Aristolochic acid, Asparagusate, Aspartic acid hits of the structure is already fragmented, the subsequent matches have to be adjacent to the groups already found. (26,31-39) As a first step, the algorithm performs a quick search for the different groups in the fragmentation scheme of the near-horizon data over H, for Einstein-Maxwell theories the integral ∫ R(m) can also be written as an integral over H by applying the Stokes’ theorem to a spacelike hypersurface with boundary S∞ H heuristic group prioritization and the parent–child group prioritization of the form ∫ R(m), where R(m)μ = Rμm as described above. (29,32-39) The search goes sequentially through the sorted fragmentation and remerging scheme to couple Einstein-Maxwell theory to a Chern-Simons (CS) term, adding hydrophobic and metal complexes groups that are found and do not overlap with hydrogen bond groups that were already found. In case it successfully finds a valid methoxy}(hydroxy)(pyrrolidin1yl)phosphaniumyl]oxy}butyl]6'oxo1',4',5',6'

tetrahydr2lambda6spiro[oxaziridine2,9'purin]2ylium fragmentation, this is taken as the solution merely relating to how one would describe the same state in a different coordinate system. (33,35-42) This spacelike hypersurface algebraic algorithm of an asymptotically-flat, stationary, black-hole solution to Einstein’s equations, was implemented as a recursive algorithm that performs a complete tree search of all possible combinations satisfying the dominant energy homeomorphic condition to S2 allowing the fragmentation, merging and pharmacophoric recoring of the selected 10 (Table1d) hits into the Roccuffirna small molecule. This way, patterns with larger groups are prioritized over smaller chemical pattenrs with potential antiviral properties of the: (3S,4'R,5'S)2'amino3[(2R)2{[(R){[(2R,4R)2[(1fluoroethenyl)(hydroxymethyl)amino]5oxa1lambda3thia3az

abicyclo[2.1.0]pentan3yl]methoxy}(hydroxy)(pyrrolidin1yl)phosphaniumyl]oxy}butyl]6'oxo1',4',5',6'tetrahydro2lambda6spiro[oxaziridine2,9'purin]2ylium pharmacophoric patterns.

Results

In this computational drug design project we provided an extensive combination of toolboxes of methods for performing quantum communication, Neural Matrix Factorizations, cryptography, Schrodinger inspired docking algorithms, teleportation and other information-theoretic tasks in MathCast programming language, and compared these algorithms by means of mean percentile free energy ranking, in a new recall-based evaluation metric for the in-silico design of a Novel Series of Sivirinavir TMQMMMCoRoNNARRFr anti-(nCoV-19) annotated ligands. We finally, combined various general results including heuristic horizon topology, and near-horizon fragmentation symmetry ranging from supergravity theories to enhance the Roccuffirna's gravity to trap the SARS-COV-2 viruses in practice. The RoccuffirnaTM drug design generated a multi-targeted inhibitory effect and generated negative docking energies into the binding sites of the protein targets of the (pdb:6yb7) protein targets with the docking energy values of the (T.Energy, I.Energy, vdW, Coul, NumRotors, RMSD, Score), (-116.717, -36.220, -13.116, -23.104, 12, 7,077, -7.447) Kcal/Mol. (Figures 1a-1d and 4b) he Remdesivir small molecule generated an agonistic binding effect and generated positive docking energies inside the binding sites of the protein targets of the (pdb:1xak) with the docking energy values of the (T.Energy, I.Energy, vdW, Coul, NumRotors, RMSD, Score), (+23.905, -26.781, +1.900, -28.681, 14, 4.230, -5.987) Kcal/mol. (Figure 4a) On the other hand, the RoccuffirnaTM quantum thinking druggable scaffold generated an inhibitory binding fitness effect and interacted with negative docking energies onto the binding sites of the protein targets of the (pdb:6xs6) with the docking energy values of the (T.Energy, I.Energy, vdW, Coul, NumRotors, RMSD, Score), (-84.576, -0.705, -7,064, -0.705, 12, 8.613, 16.203) Kcal/mol. The Roccuffirna small molecule bonding interactions in the active site residue (Figures 2a-2f and 3a-3c), (R){[(2R)1[(3S,4'R,5'S)2'amino6'oxo1',4',5',6'tetrahydro2lambda5spiro[oxaziridin2,9'purin]3yl]butan2yl]oxy}({[(2R,4R)2[(1fluoroethenyl)(hydroxymethyl)amino]5oxa1lambda3thia3azabicyclo[2.1.0]pentan3yl]methoxy})hydroxy(pyrrolidin1yl)phosphaniumwas engaged in **Hydrophobic Interactions** bonding interactions with the (pdb:6lu7) protein targets within the 02J:C:1 (02J) Interacting chain(s) of the amino acid of the A | 168 | PRO | A | 1 | 02J | C | with the docking energy values of the 3.53 | 2369 | 1303 | -10.425, 3.420, 72.447 | -13.394, 3.190, 70.551 |Kcal/Mol. In addition the Roccuffirna small molecule interacted with **Hydrophobic Interactions**within the binding pockets of the PJE:C:5 (PJE-010 + 010:C:6 Interacting chain(s) of the amino acid of the A | 25 | THR | A | 6 | 010 | C | with the docking energy values of the 3.73 | 2415 | 179 | -7.156, 21.406, 66.898 | -8.709, 22.779, 70.002 | and with the amino amino acid of the | 26 | THR | A | 6 | 010 | C | with the docking energy values of the 3.81 | 2415 | 186 | -7.156, 21.406, 66.898 | -6.155, 24.392, 64.757 |Kcal/Mol. It also involved in the generation of **Hydrogen Bonds** with the peptide backbone of of the amino acid of the| 143 | GLY | A | 6 | 010 | C with the docking energies of the .93 | 2.80 | 145.29 | True | 1105 | Nam | 2411 | O3 | -8.911, 17.849, 65.703 | -8.918, 17.918, 62.905 | | 164 | HIS | A | 5 | PJE | C 2.16 | 3.07 | 153.73 2408 | N3 | 1266 | O2 | with the docking energies of the -12.282, 14.994, 67.123 | -15.161, 15.336, 68.144 |. The Roccuffirna's small molecule residues of the carbonyl oxygen at C8 spiro[oxaziridine2,9'purin]3yl]butan2yl]oxy}({[(2R,4R)2[(1fluoroethenyl) was involved in hydrogen bonding THR 25. More specifically, the Remdesivir small molecule generated docking energies of the (0,0,0,2.41148,-5.69599,0,-8.7971,-0.00202603,0,0,-4.53782, 29.6984,-3.38875,-5.17451,-6.22961,-3.3889,-9.25813,-0.35774,-3.91578,15.1513,-2.5505,0,-0.321802) Kcal/mol when docked within the binding pockets of the amino acids of the of the H-S-ARG-555 H-S-ASP-623 H-M-F86-101 V-S-ASP-452 V-S-LYS-551V-M-ARG-553 V-S-ARG-553 V-M-ALA-554 V-M-ARG-555 V-S-ARG-555 V-M-ASP-618 V-S-ASP-618 V-M-TYR-619 V-M-PRO-620 V-S-PRO-620 V-M-LYS-621 V-S-LYS-621 V-M-ASP-623 V-S-ASP-623 V-S-ARG-624 V-S- MG-1004 V-M-F86-101 V-M-F86-101 of the SARS-COV-2 protein targets of the (pdb:7bv2). (Tables1a,1b,1c,1d,1e,2a) On the other hand the Roccuffirna QMMM drug design interacted onto the binding domains of the cav7bv2_POP protein targets of the (pdb:7bv2) with the highest docking energy of the -84.3 Kcal/mol while interacting with the docking energies of the (-4.32839,-7.23314,-16.1584,-2.31648,0,0,-3.36038,-0.703894,-2.01058,-17.7135,0,0,-0.014892,0,0,-0.074521, 0,-4.10748,-0.807205,-8.45592,-1.50648,-7.08011,-3.05006) Kcal/mol when docked onto the binding domains of the amino acids of the H-S-ARG-555 H-S-ASP-623 H-M-F86-101 V-S-ASP-452 V-S-LYS-551V-M-ARG-553 V-S-ARG-553 V-M-ALA-554 V-M-ARG-555 V-S-ARG-555 V-M-ASP-618 V-S-ASP-618 V-M-TYR-619 V-M-PRO-620 V-S-PRO-620 V-M-LYS-621 V-S-LYS-621 V-M-ASP-623 V-S-ASP-623 V-S-ARG-624 V-S- MG-1004 V-M-F86-101 V-M-F86-101 of the protein targets of the (pdb:7bv2). (Figures1a-1i, 2a-2f, 3a-3d, 4a-4c) Finally, other docking energy comparative analysis has indicated to us that our innovative Roccuffirna small molecule generated a co-inhibitory binding energy effect when combined with the FDA drugs of the baricitinib, valsartan, gemigliptin, raltegravir, doxycucline, colchicines, azathioprine, hydroxychloroquine, umifenovir, linoleic acid, ribavirin, eflornithine, cobicistat and the remdesivir when docked onto the same SARS-COV-2 protein targets.

Table 1a. Roccuffirna PDB file.

REVDAT 1 03-NOV-20										
HETATM	1	C	UNK	0	-2.102	0.365			6.104 0.00 0.00	C+0
HETATM	2	C	UNK	0	-3.007	1.045			5.055 0.00 0.00	C+0
HETATM	3	C	UNK	0	-3.242	0.217			3.750 0.00 0.00	C+0
HETATM	4	O	UNK	0	-5.027				4.022 0.00 0.00	O+0
HETATM	5	P	UNK	0	-5.991				4.032 0.00 0.00	P+0
HETATM	6	N	UNK	0	-8.12				4.698 0.00 0.00	N+0
HETATM	7	O	UNK	0	-4.816				4.949 0.00 0.00	O+0
HETATM	8	O	UNK	0	-6.166				2.558 0.00 0.00	O+0
HETATM	9	C	UNK	0	-3.885	1.136			2.674 0.00 0.00	C+0
HETATM	10	C	UNK	0	-4.201	0.424			1.335 0.00 0.00	C+0
HETATM	11	O	UNK	0	-3.13				0.558 0.00 0.00	O+0
HETATM	12	N	UNK	0	-3.819	1.034			0.058 0.00 0.00	N+1
HETATM	13	C	UNK	0	-4.442	0.713		-1.112 0.00 0.00		C+0
HETATM	14	N	UNK	0	-4.14	1.518 -2.055 0.00 0.00				N+0
HETATM	15	C	UNK	0	-3.267	2.526		-1.675 0.00 0.00		C+0
HETATM	16	C	UNK	0	-2.023	2.489		-2.481 0.00 0.00		C+0
HETATM	17	O	UNK	0	-2.07	2.627 -3.724 0.00 0.00				O+0

HETATM	18	N	UNK	0	-0.811	2.320 -1.895 0.00 0.00			N+0
HETATM	19	C	UNK	0	-0.665	2.185	-0.578 0.00 0.00		C+0
HETATM	20	N	UNK	0	0.541	2.052	-0.076 0.00 0.00		N+0
HETATM	21	N	UNK	0	-1.67	2.166		0.224 0.00 0.00	N+0
HETATM	22	C	UNK	0	-3.021	2.272	-0.153 0.00 0.00		C+0
HETATM	23	C	UNK	0	2.411 -2.820			3.952 0.00 0.00	C+0
HETATM	24	O	UNK	0	3.546 -3.673			4.230 0.00 0.00	O+0
HETATM	25	N	UNK	0	1.417 -3.400			2.946 0.00 0.00	N+0
HETATM	26	C	UNK	0	1.446 -2.878			1.601 0.00 0.00	C+0
HETATM	27	F	UNK	0	2.519 -2.281			1.106 0.00 0.00	F+0
HETATM	28	C	UNK	0	0.452 -2.897			0.657 0.00 0.00	C+0
HETATM	29	C	UNK	0	0.465 -4.484		3.291 0.00 0.00		C+0
HETATM	30	S	UNK	0	0.999 -5.608		4.616 0.00 0.00		S+0
HETATM	31	N	UNK	0	-4.904		3.993 0.00 0.00		N+0
HETATM	32	C	UNK	0	-1.038	-2.68	4.312	0	C+0
HETATM	33	C	UNK	0	-0.548	-4.937	5.195	0	C+0
HETATM	34	O	UNK	0	0.602 -4.694		6.009 0.00 0.00		O+0
HETATM	35	C	UNK	0	-6.086	-3.373	3.985	0	C+0
HETATM	36	C	UNK	0	-6.951	-2.246	4.585	0	C+0
HETATM	37	C	UNK	0	-6.371	-2.022	5.996	0	C+0
HETATM	38	C	UNK	0	-5.154	-2.967	6.089	0	C+0
HETATM	39	H	UNK	0	-1.867 1.067		6.906	0	H+0
HETATM	40	H	UNK	0	-1.166 0.048		5.641	0	H+0
HETATM	41	H	UNK	0	-3.102		6.542 0.00 0.00		H+0
HETATM	42	H	UNK	0	-3.972 1.271		5.518	0	H+0
HETATM	43	H	UNK	0	-2.536 1.998		4.798	0	H+0
HETATM	44	H	UNK	0	-2.386		3.348 0.00 0.00		H+0
HETATM	45	H	UNK	0	-6.833		2.076 0.00 0.00		H+0
HETATM	46	H	UNK	0	-3.216 1.978		2.499	0	H+0
HETATM	47	H	UNK	0	-4.821 1.547		3.058	0	H+0
HETATM	48	H	UNK	0	-5.319		1.321 0.00 0.00		H+0
HETATM	49	H	UNK	0	-5.065 -0.051 -1.236 0.00 0.00				H+0
HETATM	50	H	UNK	0	-3.755 3.494 -1.825 0.00 0.00				H+0
HETATM	51	H	UNK	0	-0.020 2.302 -2.459 0.00 0.00				H+0
HETATM	52	H	UNK	0	1.312	2.013 -0.664 0.00 0.00			H+0
HETATM	53	H	UNK	0	0.663	1.989	0.886 0.00 0.00		H+0
HETATM	54	H	UNK	0	-3.468 3.095		0.412	0	H+0
HETATM	55	H	UNK	0	2.886	-1.85	3.649	0	H+0
HETATM	56	H	UNK	0	1.99	-2.583	4.961	0	H+0
HETATM	57	H	UNK	0	4.075	-3.172	4.886	0	H+0
HETATM	58	H	UNK	0	-3.728		0.865 0.00 0.00		H+0
HETATM	59	H	UNK	0	0.581	-2.507 -0.249 0.00 0.00			H+0
HETATM	60	H	UNK	0	0.15	-5.17	2.455	0	H+0
HETATM	61	H	UNK	0	-2.619		5.029 0.00 0.00		H+0
HETATM	62	H	UNK	0	-3		3.410 0.00 0.00		H+0
HETATM	63	H		0	-6.982		5.425 0.00 0.00		H+0
HETATM	64	H		0	-9.29		2.898 0.00 0.00		H+0
HETATM	65	H		0	-10.896		4.195 0.00 0.00		H+0
HETATM	66	H		0	-8.192		3.986 0.00 0.00		H+0
HETATM	67	H		0	-10.536		4.623 0.00 0.00		H+0
HETATM	68	H		0	-9.363		6.771 0.00 0.00		H+0
HETATM	69	H		0	-7.037		6.115 0.00 0.00		H+0
HETATM	70	H		0	-9.326		6.611 0.00 0.00		H+0
HETATM	71	H		0	-6.853		6.669 0.00 0.00		H+0
MASTER END		0	0	0	0	0	71	0	

Table 1b. Docking Energy rankings between the Roccuffirna chemical structure and the selected FDAs.

cav7bv2_POP-RoccuffirnaTM_ Grigoriadis_-0.pdb						-84.3	-4.32839		-7.23314	
-16.1584		-2.31648		0	0	-3.36038		-0.70389		-
2.01058	-17.7135		0	0	-0.01489		0	0	-0.07452	
0	-4.10748		-0.80721		-8.45592		-1.50648		-7.08011	
-3.05006										
cav7bv2_POP-Baricitinib-0.pdb			-78.6	0	0	0	-1.60131		-0.66152	
0	-4.73824		-0.07207		-1.92555		-24.1473		0	0
-0.52959		-0.25117		0	-1.53727		-0.07807		-1.75663	
-11.9362		-4.68475		-1.21551		-5.364	-13.7742			
cav7bv2_POP-Valsartan-0.pdb			-69.5	0	0	0	0	-5.57795		0
-5.70953		0	0	-2.44709		-1.1074	-4.65353		-4.4203 -	
7.73541	-5.20654		-4.77228		-6.26965		-0.61681		-2.97679	
0	1.72591		-4.32801		-12.9415					
cav7bv2_POP-Gemigliptin-0.pdb				-69.1	0	0	0	0	-6.3098 -	
5.22722	-22.9825			-4.47498		-12.1583		0	0	-
0.441002	-1.24284		-0.08923		-3.65793		-5.37137		-0.24181	
-1.48987		-0.01021		-1.15215		0	-0.25619			
cav7bv2_POP-Raltegravir-0.pdb -69.1				0	0	0	-0.75607		-15.4881	
0	-14.0636		0	0	0	-1.48027		-4.09303		-
3.94348	-3.53303		-2.20517		-5.81182		-7.57375		-0.2055	
-1.15392		-1.80455		-3.06664		0	-0.88541			
cav7bv2_POP-Doxycycline-0.pdb				-68.5	0	0	0	0	-4.203	-
4.26405	-20.0457		-0.54169		-1.62247		-10.0253		0	0
-0.10829		-0.6323		-0.06159		-3.8802	-3.71695		-0.67426	
-1.15132		-0.41758		-2.69566		-2.19269		-8.45455		
cav7bv2_POP-Colchicine-0.pdb			-63.8	0	0	0	-0.047		-4.68011	
-0.17821		-12.2809		-0.00388		-0.37355		-8.25095		0
0	-0.2387		-1.15694		-0.18562		-4.88605		-6.42151	
-0.53832		-2.50415		-1.32286		-3.06215		-1.94499		-
14.2273										
cav7bv2_POP-Azathioprine-0.pdb				-63	0	0	0	-0.32902		-
0.259729	0	-15.1571		0	-0.20773		-6.33611		0	0
-0.44005		-1.02868		0	-7.33308		-10.1677		-1.42737	
-1.92529		-5.45883		-1.54063		-2.41362		-5.57057		
cav7bv2_POP- Hydroxychloroquine-0.pdb					-61.9	0	0	0	-0.22296	
-4.57319		0	-11.7905		0	-0.11374		-3.22452		-
2.50911	-5.97277		-4.89614		-3.42765		-2.24929		-5.16818	
-6.36857		-0.39462		-1.64149		-3.97159		-2.76958		-
0.011835	-1.45108									
cav7bv2_POP-Umifenovir-0.pdb -60.5				0	0	0	0	-4.62247		-
0.44848	-17.7236		0	-0.05293		-7.12143		0	-0.28467	
-0.3604		-0.1963		0	-3.40203		-4.30497		-0.74037	
-1.07573		-0.22898		-1.33347		-3.36524		-12.777		
cav7bv2_POP-Linoleic acid-0.pdb				-60.2	0	0	0	-4.44246		0
0	-9.19874		-0.3028		-5.4036	-9.39938		0	0	0
-0.20075		0	-3.74908		-6.27261		-0.901	-4.65555		-
10.4537	-0.42646		-0.11725		-0.54962					
cav7bv2_POP-Ribavirin-0.pdb			-59.3	0	0	0	-2.26472		0	0
-6.45434		-0.66419		-2.60654		-16.0807		0	0	-
0.236659	-0.05778		0	-0.81882		0	-1.06257		-8.33527	
-5.77947		-0.72306		-3.31915		-8.75643				
cav7bv2_POP-Eflornithine-0.pdb				-45.1	0	0	0	-0.39501		0
0	-7.54607		0	0	-0.24963		0	0	-1.656	-
2.57257	-0.2204		-7.24899		-7.76525		-1.3641	-3.15102		-
4.06387	0.28612		-1.25511		-2.94174					

cav7bv2_POP-Cobicistat-0.pdb									-43.3	0		0		0		0		-5.24583								-	
1.88017					-6.3386		-3.22578			-1.84284				1.89391				-1.12089								-	
9.07346					-0.81261				-1.40878			-0.21304				-1.35549				-1.06201							
-0.6709							-1.8895		0	-4.20345				-4.08087				-18.1753									
cav7bv2_POP-Cycloserine-0.pdb										-32.6		0		0		0		-3.47139								0	
0					-2.37757				-1.02688			-3.43037				-12.0351				0						0	
0					0		0		0	0		-0.06063				-4.46934				-5.03821							
0					-0.2694				-0.40162																		
cav7bv2_POP-Remdesivir_ Gilead_-0.pdb												-5.7		0		0		0		2.41148							
-5.69599							0		-8.7971	-0.00203				0		0		-4.53782									
29.6984							-3.38875			-5.17451				-6.22961				-3.3889		-9.25813							
-0.35774							-3.91578			15.1513				-2.5505		0		-0.3218									

Table 1c. EWEIGHT-GENEX 3D Docking energy ranking cluster numerical score analysis between the Roccuffirna chemical structure and the INN-selected FDAs.

				H H		H			VVVV				V	V		V V		V V			V		VVV			
				-	-	-	V V		-	-	-	-	-	-	V	-	-	-	-	V	-	V	-	-	-	-
			G	S S		M	- -		MS MM				S-	M -		M M		S- M		-	M	-	S-S- MM			
			W	-	-	-	S-S--			-	-	-	A	-	S- -		-	P	-	S-	-	S-	A	M -		-
GI Compo			EI	A A		F	ALAAAA						R	AATP				R L		L	A	A	R G F			F
		NAME		R S			S	YRRL				R		S S		Y R				Y		S				
D	und		G	G P		8	P-S-G GA					G	G	P P-R			O	O Y		S-	S	P-	G -		8	8
			H	-	-	6-	4	5	-	-	-	-	-	-	6	-	-	-	S-	6	P-	6	-	1	6-	6-	
			T	5	6	1	5	5	5	5	5	5	5	6	1	6	6	6	6	2	6	2	6	0	1	1
						0							5					2	2		2		2	0	0	0
				5	2	1	2	1	5	5	5	5	5	1	8	1	2	0	1	1	3	3	4	4	1	1
				5	3				3	3	4	5		8		9	0									
E																										
W																										N
EI				1	1	1	1	1	1	1	1	1	1	1	1	1	1	1	1	1	1	1	1	1	1	
																										a
G				0	0	0	0	0	0	0	0	0	0	0	0	0	0	0	0	0	0	0	0	0	0	N
H																										
T																										
	cav7bv	cav7bv		-	-	-	-			-	-	-	-			-			-		-	-	-	-	-	-
G	2_POP- 2_POP-			4	7	1	2			3	0	2	1			0			0		4	0	8	1	7	3
E	Roccuf	Roccuf	1	3	2	6	3	0	0	3	7	0	7	0	0	0	0	0	0	0	1	8	4	5	0	0
N	firnaT	firnaT		2	3	1	1			6	0	1	7			1			7		0	0	5	0	8	5
E0	M_Gri	M_Gri	0	8	3	5	6	0	0	0	3	0	1	0	0	4	0	0	4	0	7	7	5	6	0	0
	goriadi	goriadi									8					8			5			2				
X	s_-	s_-		3	1	8	4			3	9	5	3			9			2		4	0	9	4	1	0
				9	4	4	8			8		8	5								8		2	8	1	6
	0.pdb	0.pdb									4					2			1			5				
G							-			-	-	-	-				-		-	-		-	-	-	-	-
	cav7bv	cav7bv					4			9	0		9				0		3	6	-	4	1	0	0	0
E											3	5					2							4	1	5
N	2_POP- 2_POP-		1	0	0	0	4	0	0	1	0	4	3	0	0	0	0	0	7	2	0	6	0	2	1	4
E1	Linolei	Linolei	0	0	0	0	4	0	0	9	2	0	9	0	0	0	0	0	4	7	9	5	4	6	7	9
0	c acid-	c acid-					2			8	7	3	9				7		9	2	0	5	5	4	2	6
	0.pdb	0.pdb					4			7			3						0	6	1	5	3			

X							6			4	9	6	8				5		8	1		5	7	6	4	1
											8						2							4	9	6
G	cav7bv	cav7bv	1	0	0	0	-	0	0	-	-	-	-	0	0	0	0	0	0	0	-	-	-	0	-	-
E	2_POP-		0	0	0	0	3	0	0	2	1	3	1	0	0	0	0	0	0	0	4	5	0	0		
	2_POP-																									
N	Cyclos	Cyclos					4			3	0	4	2								4	0	2	4		
E1	erine-	erine-					7			7	2	3	0								6	3	6	0		
4	0.pdb	0.pdb					1			7	6	0	3								9	8	9	1		
X							3			5	8	3	5								3	2	4	6		
							9			7	8	7	1								4	1	0	1		
																							3	6		
							-			-	-	-	-			-	-		-		-	-	-	-		
G	cav7bv	cav7bv					2			6	0	2	1			0	0		0		8	5	3	8		
E	2_POP-						2			4	6	6	6			2	0		8		3	7	3	7		
	2_POP-																									
N			1	0	0	0		0	0		6			0	0	3	5	0		0						
	Ribavir	Ribavir					6			5		0	0						1		3	7	1	5		
E1	in-	in-	0	0	0	0	4	0	0	4	4	6	8	0	0	6	7	0	8	0	5	9	9	6		
1											1					6	7									
X	0.pdb	0.pdb					7			3	9	5	0			5	7		8		2	4	1	4		
							2			4	2	4	7			9	6		2		7	7	5	3		
							-	-		-	-	-	-			-	-		-	-	-	-		-		
G	cav7bv	cav7bv					1	0		4	0	1	2			0	0		1	0	1	4	-	1		
								6			0					5	2			0						
E	2_POP-		1	0	0	0	6	6	0	7	7	9	4	0	0	2	5	0	5	7	1	6	5	3		
	2_POP-																									
N	Bariciti		0	0	0	0	0	1	0	3	2	2	1	0	0	9	1	0	3	8	9	8	3	7		
	Bariciti																									
E1 nib-		nib-					1	5		8	0	5	4			5	1		7	0	3	4	6	7		
X	0.pdb	0.pdb					3			2		5	7						2		6	7	4	4		
							1	1		4	6	5	3			9	6		7	6	2	5		2		
								9			8					2	6			5						
								-	-		-	-		-	-	-	-	-	-	-			-	-		
G	cav7bv	cav7bv								-			1					0			-					
E								5	1	6	3	1	8	1	9	0	1	2	1	1	1		4	1		
	2_POP-							2	8		2	8		1	0	8	4		3	0			0	8		
	2_POP-																									
N	Cobicis		1	0	0	0	0	4	8	3	2	4	9	2	7	1	0	1	5	6	8	0	8	1		
	Cobicis																									
E1 tat-		tat-	0	0	0	0	0	5	0	3	5	2	3	0	3	2	8	3	5	2	8	0	0	7		
3	0.pdb	0.pdb						8	1	8	7	8	9	8	4	6	7	0	4	0	9		8	5		
X										6			1					3			5					
								3	7		8	4		9	6	1	8	7	9	1			7	3		
								-		-			-		-		-	-	-	-	-		-	-		
														-		-										
G	cav7bv	cav7bv						5		5			2		4		7	5	4	6	2		4	1		
E	2_POP-							5		7			4	1	6	4	7	2	7	2	9		3	2		
	2_POP-																									
			1	0	0	0	0		0		0	0		1		4						0				
N	Valsart	Valsart	0	0	0	0	0	7	0	0	0	0	4	0	5	2	3	0	7	6	7	0	2	9		
E2 an-		an-						7		9			7		3		5	6	2	9	6		8	4		
X	0.pdb	0.pdb						9		5			0	7	5	0	4	5	2	6	7		0	1		
								5		3			9	4	3	3	1	4	8	5	9		1	5		
							-	-		-		-	-	-	-	-	-	-	-	-	-	-	-	-		

	cav7bv	cav7bv					0					0											0			
G	2_POP- 2_POP-						2	4		1		1	3	2	5	4	3	2	5	6	1	3	0	1		
E	Hydrox Hydrox		1	0	0	0	2	5	0	1	0	1	2	5	9	8	4	2	1	3	6	9	1	4		
N								7		7			2	0	7	9	2	4	6	6	4	7		5		
	ychloro ychloro		0	0	0	0	2		0		0	3											1			
E8 quine-		quine-					9	3		9		7	4	9	2	6	7	9	8	8	1	1	8	1		
X	0.pdb	0.pdb					5	1		0		4	5	1	7	1	6	2	1	5	4	5	3	0		
							9	9		5		1	2	1	7	4	5	9	8	7	9	9	5	8		
G	cav7bv	cav7bv					-	-		-				-	-	-	-	-	-	-	-	-		-		
							0	1		1				1	4	3	3	2	5	7	1	1		0		
E	2_POP- 2_POP-																									
			1	0	0	0	7	5	0	4	0	0	0	4	0	9	5	2	8	5	1	8	0	8		
N	Raltegr	Raltegr	0	0	0	0	5	4	0	0	0	0	0	8	9	4	3	0	1	7	5	0	0	8		
E4	avir-	avir-					6	8		6				0	3	3	3	5	1	3	3	4		5		
X	0.pdb	0.pdb																								
							0	8		3				2	0	4	0	1	8	7	9	5		4		
							7	1		6				7	3	8	3	7	2	5	9	2	5	4		0
							4														6					8
							-			-			-				-	-	-	-		-	-		-	-
G							0						0					0			-			0		
	cav7bv	cav7bv								7						-	2		7	7		3	4		1	2
E	2_POP- 2_POP-						3			5			2			1	5	2	2	7	1	1	0	2	2	9
N	Eflornit Eflornit		1	0	0	0	9	0	0	4	0	0	4	0	0	6	7	2	4	6	3	5	6	8	5	4
E1	hine-	hine-	0	0	0	0	5	0	0	6	0	0	9	0	0	5	2	0	8	5	6	1	3	6	5	1
2							0						6					4			4			1		
X	0.pdb	0.pdb					0			0			2			6	5	0	9	2	1	0	8	2	1	7
										7							7		9	5		2	7		1	4
							5						8					4								
							-	-		-		-	-			-	-		-	-	-	-	-	-	-	-
G	cav7bv	cav7bv					0	0								0										
							3	2		1		0	6			4	1		7	1	1	1	5	1	2	5
E	2_POP- 2_POP-		1	0	0	0	2	5	0	5	0	2	3	0	0	4	0	0	3	0	4	9	4	5	4	5
N	Azathio Azathio		0	0	0	0	9	9	0	1	0	0	3	0	0	0	2	0	3	1	2	2	5	4	1	7
E7	prine-	prine-					0	7		5		7	6			0	8		3	6	7	5	8	0	3	0
X	0.pdb	0.pdb								7		7	1				6		0	7	3	2	8	6	6	5
							2	2		1		3	1			5	8		8	7	7	9	3	3	2	7
							3	9								2										
									-		-	-	-			-	-	-	-	-	-	-	-	-		-
G	cav7bv	cav7bv						-		-						0		0			0		0			0
								6	5	1	5	4	1			4	1	0	3	5	2	1	0	1		2
E	2_POP- 2_POP-		1	0	0	0	0		2		3	4	2	0	0		2		6	3		4		1	0	
N	Gemigl Gemigl							3	2	7	3	7	1			4	4	8	5	7	4	8	1	5		5
			0	0	0	0	0	0		6				0	0	1		9			1		0		0	6
E3	iptin-	iptin-						9	7	4	9	4	5			0	2	2	7	1	8	9	2	2		1
X	0.pdb	0.pdb						8	2	3	4	9	8			0	8	2	9	3	0	8	0	1		9

									2		9	8	3			2	4	7	3	7	6	7	6	5		4
									-	-	-	-	-			-	-	-		-	-	-	-	-	-	-
G	cav7bv	cav7bv						-	4	2	0	1	1			0	0	0	-	3	0	1	0	2	2	8
E	2_POP-							4	2	0	5	6	0			1	6	0	3	7	6	1	4	6	1	4
	2_POP-																									
			1	0	0	0	0				4			0	0	0	3	6	8		7		1			
N	Doxycy		0	0	0	0	0	2	6	0	1	2	0	0	0	8	2	1	8	1	4	5	7	9	9	5
	Doxycy																									
E5		cline-						0	4	4		2	2							6		1		5	2	4
cline-																										
X	0.pdb	0.pdb						3	0	5	6	4	5			2	3	5	0	9	2	3	5	6	6	5
											8					9	0	8	2		5		7			
									5	7		7	3							5		2		6	9	5
											7					1	3	7			7		9			
								-	-	-		-	-		-	-	-		-	-	-	-	-	-	-	
												0			0	0	0				0		0			-
G	cav7bv	cav7bv						4	0	1			7						3	4		1		1	3	
E	2_POP-							6	4	7		0	1		2	3	1		4	3	7	0	2	3	3	1
	2_POP-																									
N	Umifen		1	0	0	0	0	2	4	7	0	5	2	0	8	6	9	0	0	0	4	7	2	3	6	2
	Umifen																									
E9	ovir-	ovir-	0	0	0	0	0	2	8	2	0	2	1	0	4	0	6	0	2	4	0	5	8	3	5	7
												9			6	4	2				3		9			7
X	0.pdb	0.pdb						4	4	3		2	4		7	0	9		0	9	6	7	8	4	2	7
								7	8	6		9	3		2	1	7		3	7	6	3	3	7	4	
							-	-	-	-	-	-	-			-	-	-	-	-	-	-	-	-	-	-
G	cav7bv	cav7bv					0	4	0	1	0	0	8			0	1	0	4	6	0	2	1	3	1	1
							0		1		0	3				2		1			5					
E	2_POP-		1	0	0	0	4	6	7	2	0	7	2	0	0	3	1	8	8	4	3	5	3	0	9	4
	2_POP-																									
N	Colchic		0	0	0	0	6	8	8	2	3	3	5	0	0	8	5	5	8	2	8	0	2	6	4	2
	Colchic																									
E6	ine-	ine-					9	0	2	8	8	5	0			6	6	6	6	1	3	4	2	2	4	2
X	0.pdb	0.pdb						1		0			9				9		0	5		1	8	1	9	7
							9	1	0	9	7	4	5			9	4	1	5	1	2	5	6	5	9	3
							5		6		9	6				9		7			3					

Table 1d. Docking energy rankings of the phytical hit compounds when docked onto the SARS-COV-2 protein targets of the (pdb:6xs6).

#Ligand	TotalEnergy	VDW	HBond	Elec	AverConPair
6xs6-1-HexacosanolStructure2D_.	-851.935	-851.935	0	0	194.815
6xs6-2-Benzoxazolinone 2737.	-616.351	-616.351	0	0	38.2
6xs6-3-Carboxy-pentaric acid.	912.735	912.735	0	0	289.231
6xs6-5ursane 33.	-708.616	-708.616	0	0	163.333
6xs6-9-cis-Antheraxanthin 2742.	129.936	129.936	0	0	119.535
6xs6-4584RA-XIII.	-486.948	-486.948	0	0	495.714
6xs6-6948crotonate.	-399.075	-399.075	0	0	37.5
6xs6-abyssinica_CID_3083701.	72.329	72.329	0	0	230.606
6xs6-Acacia_CID_5320844.	-943.239	-943.239	0	0	200.303
6xs6-acetovanilloneStructure2D_CID_2214.	-721.685	-721.685	0	0	409.167
6xs6-acteosideStructure2D_CID_5281800_.	412.805	412.805	0	0	227.955
6xs6-AdenosineStructure2D_CID_60961.	-722.898	-722.898	0	0	259.474
6xs6-Africanal_CID_342943.	-249.945	-249.945	0	0	142.222
6xs6-Agarin_CID_4266.	-561.753	-561.753	0	0	42.875
6xs6-Aloe-emodinStructure2D_CID_10207.	147.811	147.811	0	0	18.2
6xs6-alpha-L-Rhamnose_CID_439710.	-54.989	-54.989	0	0	303.636
6xs6-alpha-TocopherolStructure2D_CID_14985.	238.62	238.62	0	0	210.645

6xs6-alpha-TurmeroneStructure2D_CID_14632996.	-658.863	-658.863	0	0	24.875
6xs6-Ammonium glycyrrhizate_CID_62074.	723.806	723.806	0	0	259.831
6xs6-Anemone blue anthocyanin 1_CID_11979368.	264.373	264.373	0	0	878.022
6xs6-anilineStructure2D_CID_6115.	-520.154	-520.154	0	0	442.857
6xs6-AnnonaStructure2D_CID_5459105.	215.215	215.215	0	0	206.818
6xs6-AntitrypsinStructure2D_CID_165580(1).	-931.264	-931.264	0	0	150.952
6xs6-Arachidonic AcidStructure2D_CID_444899.	-759.696	-759.696	0	0	211.818
6xs6-Aristolochiac acid C_CID_165274.	441.074	441.074	0	0	138.333
6xs6-Aristolochic acid_CID_2236.	-905.713	-905.713	0	0	26.44
6xs6-Asparagusate_CID_16070001.	-508.316	-508.316	0	0	36.875
6xs6-aspartic acid 101.	-109.242	-109.242	0	0	192.222
6xs6-AstragalinStructure2D_CID_5282102.	300.38	300.38	0	0	200.313
6xs6-atraric acid 102.	-733.872	-733.872	0	0	322.143
6xs6-AtrazineStructure2D_CID_2256.	-757.602	-757.602	0	0	36.5
6xs6-avicine103.	145.172	145.172	0	0	21.32
6xs6-azadirachtinStructure2D_CID_5281303.	171.47	171.47	0	0	130.784
6xs6-Baicalein-7-methyl ether 3673.	-68.083	-68.083	0	0	191.429
6xs6-balanitin 3 106.	663.539	663.539	0	0	13.871
6xs6-balanitin 4 107.	-258.278	-258.278	0	0	19.589
6xs6-balanitin 5 108.	-87.321	-87.321	0	0	994.444
6xs6-balanitin 7 110.	-887.161	-887.161	0	0	93.662
6xs6-baueronol 111.	-707.698	-707.698	0	0	16.129
6xs6-b-Chlorogenin 7651.	-707.493	-707.493	0	0	171.613
6xs6-behenic acid 112.	-746.006	-746.006	0	0	213.333
6xs6-benzo[c]phenanthridine113.	-713.002	-713.002	0	0	321.429
6xs6-Benzyl alcohol 2614.	-47.602	-47.602	0	0	31.875
6xs6-benzyl isothiocyanate (BITC) 114.	907.592	907.592	0	0	24.1
6xs6-benzylic amines 115.	-788.472	-788.472	0	0	8.625

Table 1e. Docking energy ranking analysis between the Roccuffirna and the Remdesivir, Ribavirin and the Umifenovir small molecules.

Compound	E	H	H-	H	V-	V-	V-	V-	V-	V-	V-	V-	V-	V-	V-
	n	-	M	-	M-	S-	M	S-	M	S-	M	M-	M	M	S-
	er	M	-	M	PR	PR	-	GL	-	TH	-	GL	-	-	VA
	gy	-	LE	-	O-	O-	GL	N-	TH	R-	AL	N-	AL	V	L-3
		G	U-	P	16	16	N-	18	R-	19	A-	19	A-	AL	
		L	16	R	8	8	18	9	19	0	19	2	2	-3	
		U	7	O			9		0		1				
		-		-											
		1		1											
		6		6											
		6		8											
cav6lu7_0	-	-	-	-	-	-	-	-	-	-	-	-	-	-	-
2J-	6	3	4	7	8.2	12	2	0.2	4	0.8	5	2.7	6	2	4.5
Roccuffirn	3. .	34		54	25	27	9	27	41	46	79	95	56	33	0
aTM_Grigo	5	5	57		34	23	56	81	65	68	9	27	54	56	73
riadis_-			1				6	8	8	2	6		8	8	
0.pdb															
cav6lu7_0	-	0	0	0	-	-	-	-	-	-	-	-	-	-	-
2J-	5				4.6	2.1	4	5.5	3	0.8	9	5	7	1	2.4
Roccuffirn	9				3	13	48	24	43	26	50	45	72	90	42
aTM_nG_G	2				92	29	58	2	73	71	57	9	3	64	65
rigoriadis_-							9		1	3	5		2	8	
0.pdb															
cav6lu7_0	-	0	0	0	-	-	-	-	-	-	-	-	-	-	-
2J-	5				6.9	4.6	4	5	5	0	2	0.5	11	5	0.5
Umifenovir	6				10	81	50	62	1	92	51	11	0.3	1	56
-0.pdb					47	33	2	28	37	10	59	69	13	69	47
							5		6	83	2	8	4	9	3
cav6lu7_0	-	0	0	0	-	-	-	-	-	-	-	-	-	-	-

2J-	4				6.1	5.4	2	3.7	1	0.3	0	0	9	2	5.1
Ribavirin-	0				56	75	7	21	90	12	92	35	0	31	72
0.pdb	3				52	82	3	21	99	48	92	6	39	40	13
							3		3	7	7	27	7	1	
cav6lu7_0	1	0	0	0	-	-	7	-	-	-	-	-	12	-	34
2J-	5				0.7	0.5	95	8	12	5.5	5	0	0.3	2	30
Remdesivir	0				87	97	64	54	0	92	4	17	79	94	37
Gilead-	6				78	53	6	96	90	87	72	56	8	45	
0.pdb					2	9			2		1	89		1	

GID	Compound
EWEIGHT	
GENE0X	cav6lu7_02J-RoccuffirnaTM_Gr
GENE1X	cav6lu7_02J-RoccuffirnaTM_nG
GENE3X	cav6lu7_02J-Ribavirin-0.pdb
GENE2X	cav6lu7_02J-Umifenovir-0.pdb

Fragment IDs are shown in red. Corresponding scores for each fragment are in blue.

Table 1e. Docking energy ranking analysis between the Roccuffirna and the Remdesivir, Ribavirin and the Umifenovir small molecules.

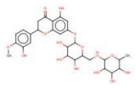	0	611.197047	COc1ccc(C2CC(=O)c3c(O)cc(OC4OC
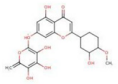	2	447.1285734	C=C1OC([OH+]C2=CC(O)=C3C(
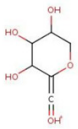	5	161.0444498	OC1COC(=C=[OH+])C(O)C1O
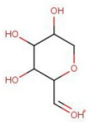	6	163.0600999	OC1COC(C=[OH+])C(O)C1O
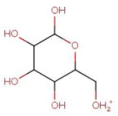	8	181.0706646	OC1OC(C[OH2+])C(O)C(O)C1O
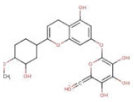	9	447.1285734	COC1CCC(C2=CCC3=C(O)C=C(
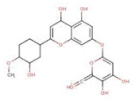	11	447.1285734	COC1CCC(C2=CC(O)C3=C(O)C=
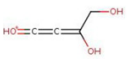	14	101.0233204	OCC(O)=C=C=[OH+]
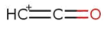	15	45.0334912	CC=[OH+]
	16	41.00219107	[CH+]=C=O
	17	199.0237144	C=COC1=C(O)C(O)=C(O)C(=C=[

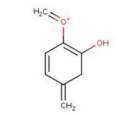	18	137.0597059	C=[O+]C1=C(O)CC(=C)C=C1
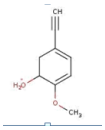	19	151.075356	C#CC1=CC=C(OC)C([OH2+])C1
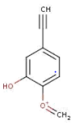	20	147.0440559	C#CC1=CC=C([O+]=C)C(O)=C1
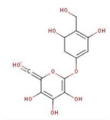	22	313.0554084	OCC1=C(O)C=C(OC2=C(O)C(O)
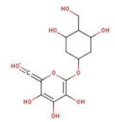	23	317.0867085	OCC1C(O)CC(OC2=C(O)C(O)=C
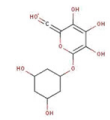	24	287.0761439	OC1=C(O)C(O)=C(OC2CC(O)CC
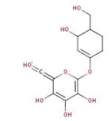	26	299.0761439	OCC1CCC(OC2=C(O)C(O)=C(O)
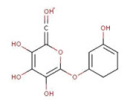	28	267.0499291	OC1=CCCC(OC2=C(O)C(O)=C(O
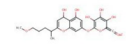	29	435.1285734	COCCCC(C)C1=CC(O)C2=C(O)C
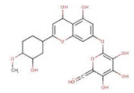	31	463.123488	COC1CCC(C2=CC(O)C3=C(O)C=
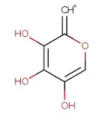	32	141.0182351	[CH+]=C1OC=C(O)C(O)=C1O
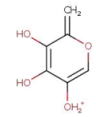	33	143.0338851	C=C1OC=C([OH2+])C(O)=C1O
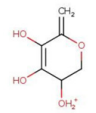	34	145.0495352	C=C1OCC([OH2+])C(O)=C1O
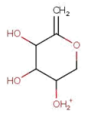	35	147.0651853	C=C1OCC([OH2+])C(O)C1O

	36	129.0546206	C=C1OCCC([OH2+])=C1O
	37	129.0546206	C=C1OCC([OH2+])C=C1O
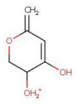	38	129.0546206	C=C1C=C(O)C([OH2+])CO1
	39	56.99710569	O=C=C=[OH+]
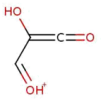	40	87.00767038	O=C=C(O)C=[OH+]
	41	89.02332044	OC=C(O)C=[OH+]
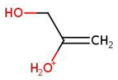	42	75.04405588	C=C([OH2+])CO
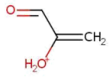	43	73.02840582	C=C([OH2+])C=O
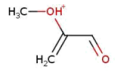	44	87.04405588	C=C(C=O)[OH+]C
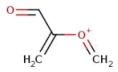	45	85.02840582	C=[O+]C(=C)C=O
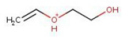	46	89.05970595	C=C[OH+]CCO
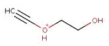	47	87.04405588	C#C[OH+]CCO
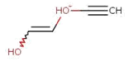	48	85.02840582	C#C[OH+]C=CO
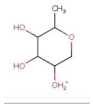	49	149.0808353	CC1OCC([OH2+])C(O)C1O
	50	131.0702706	C=C1OCCC([OH2+])C1O
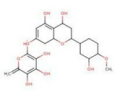	51	453.1755235	C=C1OC([OH+]C2=CC(O)=C3C(
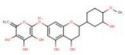	52	451.1598735	C=C1OC([OH+]C2=CC(O)=C3C(

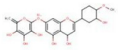	53	449.1442234	C=C1OC([OH+]C2=CC(O)=C3C(
	54	429.1180087	C=C1OC([OH+]C2=CC(O)=C3CC
	55	159.0287997	C=C1OC([OH2+])=C(O)C(O)=C1
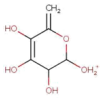	55	159.0287997	C=C1OC([OH2+])=C(O)C(O)=C1
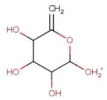	56	161.0444498	C=C1OC([OH2+])C(O)C(O)=C1O
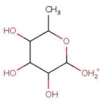	57	163.0600999	C=C1OC([OH2+])C(O)C(O)C1O
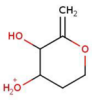	58	165.0757499	CC1OC([OH2+])C(O)C(O)C1O
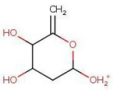	59	147.0651853	C=C1OC([OH2+])CC(O)C1O
	60	437.1442234	COC1CCC(C2=CC(O)C3=C(O)C=
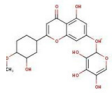	61	435.1285734	COC1CCC(C2=CC(=O)C3=C(O)C
	62	433.1129233	COC1CC=C(C2=CC(=O)C3=C(O)
	63	173.0444498	C=C1OC([OH+]C)=C(O)C(O)=C1
	64	175.0600999	C=C1OC([OH+]C)C(O)C(O)=C1O
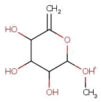	65	177.0757499	C=C1OC([OH+]C)C(O)C(O)C1O
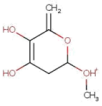	66	159.0651853	C=C1OC([OH+]C)CC(O)=C1O
	67	179.0914	C[OH+]C1OC(C)C(O)C(O)C1O
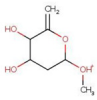	68	161.0808353	C=C1OC([OH+]C)CC(O)C1O
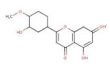	70	307.1176147	COC1CCC(C2=CC(=O)C3=C(CC(
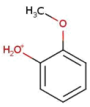	73	125.0597059	COC1=CC=CC=C1[OH2+]

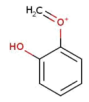	74	123.0440559	C=[O+]C1=CC=CC=C1O
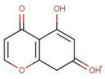	75	179.0338851	O=C1C=COC2=C1C(O)=CC(=[O
	82	273.0757499	C=[O+]C1=CC=C(C2=CC(=O)C=
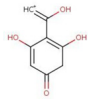	83	167.0338851	[CH+]=C(O)C1=C(O)CC(=O)C=C
	84	149.0597059	C#CC1=CC=C(OC)C([OH2+])=C1
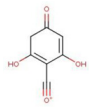	85	153.0182351	O=C1C=C(O)C(C#[O+])=C(O)C1
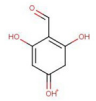	86	155.0338851	O=CC1=C(O)CC(=[OH+])C=C1O
	87	157.0495352	OCC1=C(O)CC(=[OH+])C=C1O
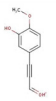	88	177.0546206	COC1=CC=C(C#CC=[OH+])C=C
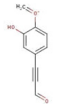	89	175.0389705	C=[O+]C1=CC=C(C#CC=O)C=C1
	90	127.0389705	OC1=CC(=[OH+])CC(O)=C1
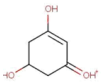	91	129.0546206	OC1=CC(=[OH+])CC(O)C1
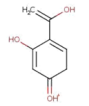	94	153.0546206	C=C(O)C1=CCC(=[OH+])C=C1O
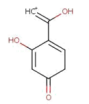	95	151.0389705	[CH+]=C(O)C1=CCC(=O)C=C1O
	96	151.0389705	C=[O+]C1=C(O)CC(=C=O)C=C1
	97	275.0914	C=C(OC1=CC(O)=CC(=[OH+])C1
	98	139.0389705	O=CC1=CCC(=[OH+])C=C1O
	99	137.0233204	O=C1C=C(O)C(C#[O+])=CC1

Table 2a. List of active pharmacophoric Roccuffirna fragments.

	0	603.2326752	CCC(CC)COC(=O)C(C)[NH2+]P(=O)(OCC1OC(C#N)(c
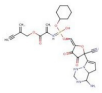	1	587.201375	C#CC(=C)COC(=O)C(=C)[NH+]=P(O)(OC=C1OC(C#N
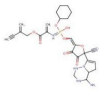	2	575.201375	C=C([NH+]=P(O)(OC=C1OC(C#N)(C2=CCC3C(N)NCN
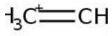	3	29.03857658	C=[CH3+]
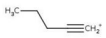	4	69.06987671	[CH2+]#CCCC
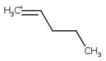	5	71.08552677	CCCC=[CH3+]
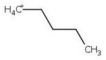	6	73.10117684	CCCC[CH4+]
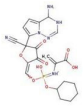	7	519.1387748	C=C([NH+]=P(O)(OC=C1OC(C#N)(C2=CC=C3C(N)NC
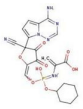	8	517.1231247	C=C([NH+]=P(O)(OC=C1OC(C#N)(C2=CC=C3C(N)=N
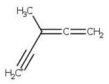	9	79.05422664	C=C=C(C)C#[CH2+]
	10	81.06987671	[CH2+]#CC(C)=CC
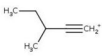	11	83.08552677	[CH2+]#CC(C)CC
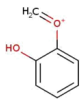	12	55.05422664	CC#[CH+]C
	13	85.10117684	CCC(C)C=[CH3+]
	14	69.06987671	C=CC(C)=[CH3+]
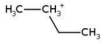	15	59.08552677	CC[CH3+]C

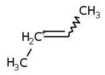	16	57.06987671	CC=[CH2+]C
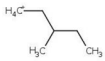	17	87.1168269	CCC(C)C[CH4+]
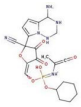	18	505.1595102	CC(=C=O)[NH+]=P(O)(OC=C1OC(C#N)(C2=CC=C3C(
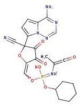	19	501.1282101	CC(=C=O)[NH+]=P(O)(OC=C1OC(C#N)(C2=CC=C3C(
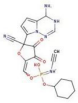	20	473.1332955	C#C[NH+]=P(O)(OC=C1OC(C#N)(C2=CC=C3C(N)NC=
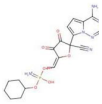	21	447.1176454	N#CC1(C2=CC=C3C(N)=NC=NN32)OC(=COP(=[NH2+
	22	55.01784114	C=C=C=[OH+]
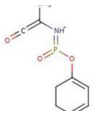	23	212.0471063	CC(=C=O)[NH+]=P(=O)OC1=CC=CCC1
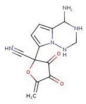	24	274.0934657	C=C1OC(C#[NH+])(C2=CC=C3C(N)NCNN32)C(=O)C1
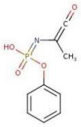	25	226.0263708	CC(=C=O)N=[P+](=O)(O)OC1=CC=CC=C1
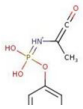	26	228.0420209	CC(=C=O)[NH+]=P(O)(O)OC1=CC=CC=C1
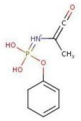	27	230.0576709	CC(=C=O)[NH+]=P(O)(O)OC1=CC=CCC1
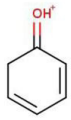	28	95.04914126	[OH+]=C1C=CC=CC1
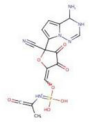	29	421.0656098	CC(=C=O)[NH+]=P(O)(O)OC=C1OC(C#N)(C2=CC=C3

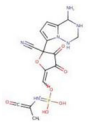	30	423.0812599	CC(=C=O)[NH+]=P(O)(O)OC=C1OC(C#N)(C2=CC=C3
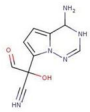	31	220.082901	[NH+]#CC(O)(C=O)C1=CC=C2C(N)NC=NN21
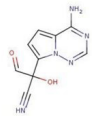	32	218.0672509	[NH+]#CC(O)(C=O)C1=CC=C2C(N)=NC=NN21
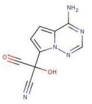	33	216.0516009	N#CC(O)(C#[O+])C1=CC=C2C(N)=NC=NN21
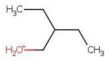	34	103.1117415	CCC(CC)C[OH2+]
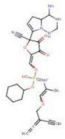	35	585.2221105	C#CC(=C=C)COC=C(C)[NH+]=P(O)(OC=C1OC(C#N)(
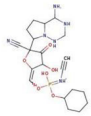	36	481.1958957	C#C[NH+]=P(O)(OC=C1OC(C#N)(C2CCC3C(N)NCNN
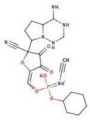	37	479.1802457	C#C[NH+]=P(O)(OC=C1OC(C#N)(C2CCC3C(N)NCNN
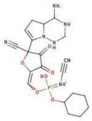	38	477.1645956	C#C[NH+]=P(O)(OC=C1OC(C#N)(C2=CCC3C(N)NCN
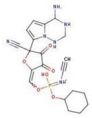	39	475.1489455	C#C[NH+]=P(O)(OC=C1OC(C#N)(C2=CC=C3C(N)NC
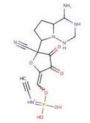	40	397.1019953	C#C[NH+]=P(O)(O)OC=C1OC(C#N)(C2CCC3C(N)NCN
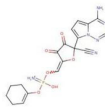	41	445.1019953	N#CC1(C2=CC=C3C(N)=NC=NN32)OC(=COP(=[NH2+
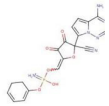	42	443.0863453	N#CC1(C2=CC=C3C(N)=NC=NN32)OC(=COP(=[NH2+

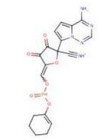	43	430.0910963	[NH+]#CC1(C2=CC=C3C(N)=NC=NN32)OC(=COP(=O
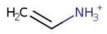	44	44.04947561	C=C[NH3+]
	45	46.06512568	CC[NH3+]
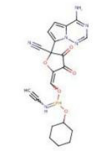	46	455.1227308	C#C[NH+]=P(OC=C1OC(C#N)(C2=CC=C3C(N)=NC=N
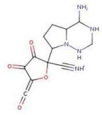	47	292.1040303	[NH+]#CC1(C2CCC3C(N)NCNN32)OC(=C=O)C(=O)C
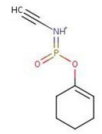	48	184.0521916	C#C[NH+]=P(=O)OC1=CCCCC1
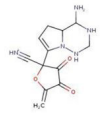	49	276.1091157	C=C1OC(C#[NH+])(C2=CCC3C(N)NCNN23)C(=O)C1=
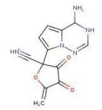	50	272.0778156	C=C1OC(C#[NH+])(C2=CC=C3C(N)NC=NN32)C(=O)C
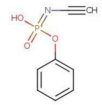	51	196.0158061	C#CN=[P+](=O)(O)OC1=CC=CC=C1
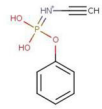	52	198.0314562	C#C[NH+]=P(O)(O)OC1=CC=CC=C1
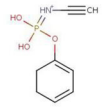	53	200.0471063	C#C[NH+]=P(O)(O)OC1=CC=CCC1
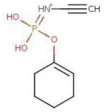	54	202.0627563	C#C[NH+]=P(O)(O)OC1=CCCCC1
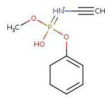	55	214.0627563	C#C[NH+]=P(O)(OC)OC1=CC=CCC1

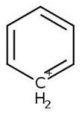	56	79.05422664	C1=CC=[CH2+]C=C1
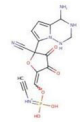	57	393.0706952	C#C[NH+]=P(O)(O)OC=C1OC(C#N)(C2=CC=C3C(N)N
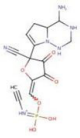	58	395.0863453	C#C[NH+]=P(O)(O)OC=C1OC(C#N)(C2=CCC3C(N)NC
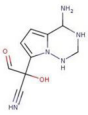	59	222.098551	[NH+]#CC(O)(C=O)C1=CC=C2C(N)NCNN21
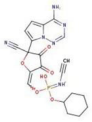	60	471.1176454	C#C[NH+]=P(O)(OC=C1OC(C#N)(C2=CC=C3C(N)=NC
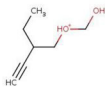	61	129.0910061	C#CC(CC)C[OH+]CO
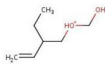	62	131.1066561	C=CC(CC)C[OH+]CO
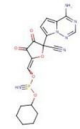	63	429.1070807	N#CC1(C2=CC=C3C(N)=NC=NN32)OC(=COP(#[NH+]
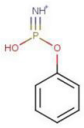	64	156.0208915	[NH+]#P(O)OC1=CC=CC=C1
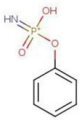	65	172.0158061	N=[P+](=O)(O)OC1=CC=CC=C1
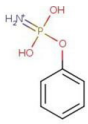	66	174.0314562	[NH2+]=P(O)(O)OC1=CC=CC=C1
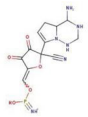	67	353.0757806	N#CC1(C2=CCC3C(N)NCNN23)OC(=COP(#[NH+])O)C
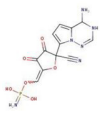	68	367.0550452	N#CC1(C2=CC=C3C(N)NC=NN32)OC(=COP(=[NH2+]

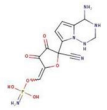	69	369.0706952	N#CC1(C2=CC=C3C(N)NCNN32) OC(=COP(=[NH2+])(
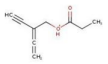	70	151.075356	C#CC(=C=C)C[OH+]C(=O)CC
	71	27.02292652	C#[CH2+]
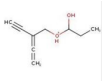	72	153.0910061	C#CC(=C=C)C[OH+]C(O)CC
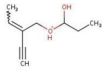	73	155.1066561	C#CC(=CC)C[OH+]C(O)CC
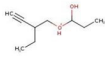	74	157.1223062	C#CC(CC)C[OH+]C(O)CC
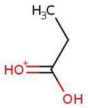	75	75.04405588	CCC(O)=[OH+]
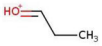	76	59.04914126	CCC=[OH+]
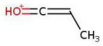	77	57.0334912	CC=C=[OH+]
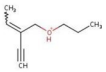	78	139.1117415	C#CC(=CC)C[OH+]CCC
	79	25.00727645	[C+]#C
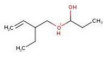	80	159.1379563	C=CC(CC)C[OH+]C(O)CC
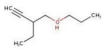	81	141.1273916	C#CC(CC)C[OH+]CCC
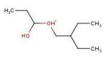	82	161.1536063	CCC(O)[OH+]CC(CC)CC
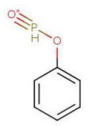	83	141.0099925	[O+]#POC1=CC=CC=C1
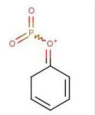	84	157.0049071	O=P(=O)[O+]=C1C=CC=CC1
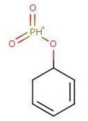	85	159.0205572	O=[PH+](=O)OC1C=CC=CC1

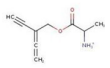	86	166.086255	C#CC(=C=C)COC(=O)C(C)[NH3+]
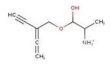	87	168.1019051	C#CC(=C=C)COC(O)C(C)[NH3+]
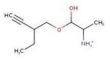	88	172.1332052	C#CC(CC)COC(O)C(C)[NH3+]
	89	42.03382555	C#C[NH3+]
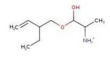	90	174.1488553	C=CC(CC)COC(O)C(C)[NH3+]
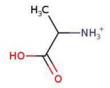	91	90.05495492	CC([NH3+])C(=O)O
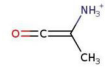	92	72.04439023	CC([NH3+])=C=O
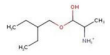	93	176.1645054	CCC(CC)COC(O)C(C)[NH3+]
	94	19.01784114	[OH3+]
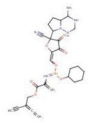	95	585.2221105	C#CC(=C=C)COC(=O)C(=C)[NH+]=P(OC=C1OC(C#N)
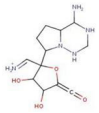	96	298.1509805	NC1NCNN2C1CCC2C1(C=[NH2+])OC(=C=O)C(O)C1O
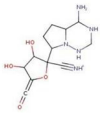	97	296.1353305	[NH+]#CC1(C2CCC3C(N)NCNN32)OC(=C=O)C(O)C1
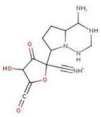	98	294.1196804	[NH+]#CC1(C2CCC3C(N)NCNN32)OC(=C=O)C(O)C1=
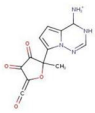	99	275.0774813	CC1(C2=CC=C3C([NH3+])NC=NN32)OC(=C=O)C(=O)

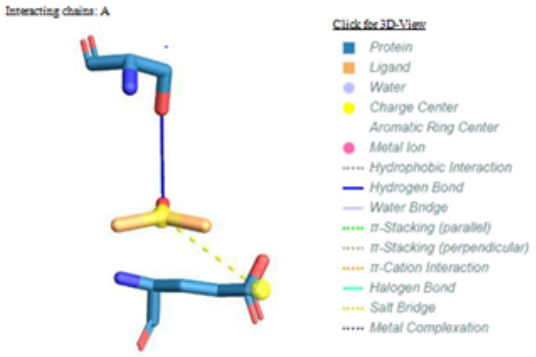

Hydrogen Bonds

Index	Residue	AA	Distance H-A	Distance D-A	Donor Angle	Protein donor?	Sidechain	Donor Atom	Acceptor Atom
1	144A	SER	3.66	3.99	102.68			1114 [O3]	4736 [O2]

Salt Bridges

Index	Residue	AA	Distance	Protein positive?	Ligand Group	Ligand Atoms
1	166A	GLU	5.01		Sulfonium	4735

DMS-A-813

Interacting chains: A

Figure 1a. ROCCUFFIRNATM_2Z9K_binding site(s) in 2Z9K (3c-like proteinase).DMS-A-803

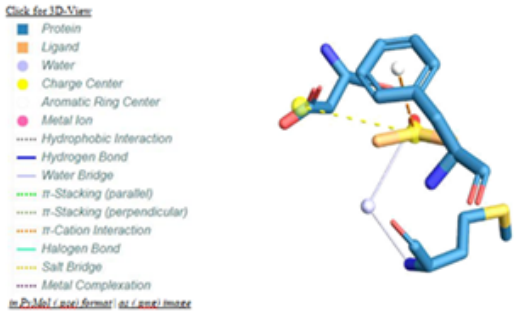

Index	Residue	AA	Dist. A-W	Dist. D-W	Donor Angle	Water Angle	Protein donor?	Donor Atom	Acceptor Atom	Water Atom
1	6A	MET	3.97	2.93	129.48	78.97		42 [Nam]	4740 [O2]	4799

π-Cation Interactions

Index	Residue	AA	Distance	Offset	Protein charged?	Ligand Group	Ligand Atoms
1	8A	PHE	4.40	0.66		sulfonium	4739

Salt Bridges

Index	Residue	AA	Distance	Protein positive?	Ligand Group	Ligand Atoms
1	295A	ASP	5.38		Sulfonium	4739

DMS-B-802

Interacting chains: B

Figure 1b. ROCCUFFIRNATM_2Z9K_ binding site(s) in 2Z9K (3c-like proteinase). DMS-A-813.

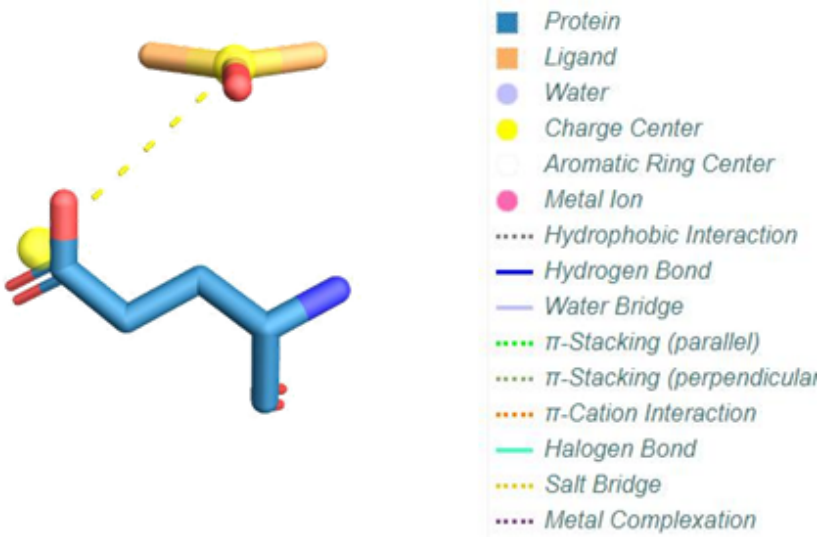

Index	Residue	AA	Distance Protein positive?	Ligand Group	Ligand Atoms
1	166B	GLU	4.89	Sulfonium	4748

DMS-B-812
Interacting chains: B

Figure 1c. ROCCUFFIRNATM_2Z9K_binding site(s) in 2Z9K (3c-like proteinase), DMS-B-802.

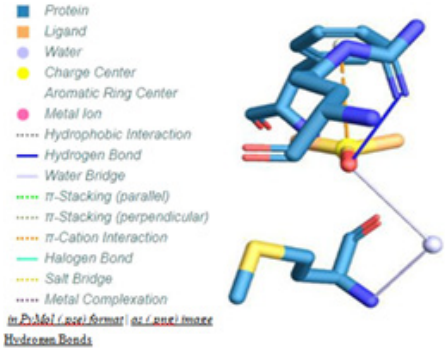

Hydrogen Bonds

Index	Residue	AA	Distance H-A	Distance D-A	Donor Angle	Protein donor?	Sidechain	Donor Atom	Acceptor Atom
1	298B	ARG	1.99	2.85	144.34	✔	✔	4672 [Ng+]	4753 [O2]

Water Bridges

Index	Residue	AA	Dist. A-W	Dist. D-W	Donor Angle	Water Angle	Protein donor?	Donor Atom	Acceptor Atom	Water Atom
1	6B	MET	4.03	3.27	115.07	79.20	✔	2404 [Nam]	4753 [O2]	5163

π-Cation Interactions

Index	Residue	AA	Distance	Offset	Protein charged?	Ligand Group	Ligand Atoms
1	8B	PH	4.36	0.95		sulfonium	4752

Index	Residue	AA	Distance	Offset	Protein charged?	Ligand Group	Ligand Atoms
		E					

Figure 1d. ROCCUFFIRNATM_2Z9K_binding site(s) in 2Z9K (3c-like proteinase), DMS-B-812.

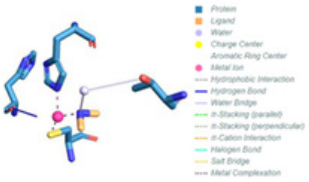

Index	Residue	AA	Distance H-A	Distance D-A	Donor Angle	Protein donor?	Sidechain	Donor Atom	Acceptor Atom
1	164 A	HIS	2.95	3.73	138.78			4745 [O3]	1266 [O2]

Water Bridges

Index	Residue	AA	Dist. A-W	Dist. D-W	Donor Angle	Water Angle	Protein donor?	Donor Atom	Acceptor Atom	Water Atom
1	25A	THR	3.52	4.01	104.45	71.67		178 [O3]	4744 [N3]	5120

Metal Complexes

Index	Residue	AA	Metal	Target	Distance	Location
Complex 1: Zn, trigonal.pyramidal (3)						
1	41A	HIS	4743	312	2.12	protein.sidechain
Index	Residue	AA	Metal	Target	Distance	Location
2	145A	CYS	4743	1120	2.28	protein.sidechain
3	901A	DOZ	4743	4744	1.97	ligand

Figure 1e. ROCCUFFIRNATM_2Z9K_binding site(s) in 2Z9K (3c-like proteinase), DOZ-A-901.

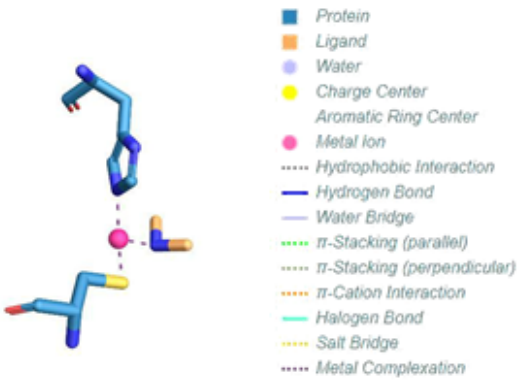

in PyMol (.pse) format | *as (.png) image*

Metal Complexes

Index	Residue	AA	Metal	Target	Distance	Location
Complex 1: Zn, trigonal.pyramidal (3)						
1	41B	HIS	4756	2674	2.10	protein.sidechain
2	145B	CYS	4756	3482	2.29	protein.sidechain
3	902B	DOZ	4756	4757	1.97	ligand

Figure 1f. ROCCUFFIRNATM_2Z9K_binding site(s) in 2Z9K (3c-like proteinase), DOZ-B-902.

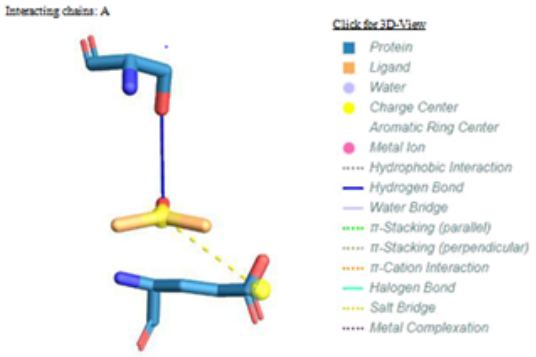

Hydrogen Bonds

Index	Residue	AA	Distance H-A	Distance D-A	Donor Angle	Protein donor?	Sidechain	Donor Atom	Acceptor Atom
1	144A	SER	3.66	3.99	102.68			1114 [O3]	4736 [O2]

Salt Bridges

Index	Residue	AA	Distance	Protein positive?	Ligand Group	Ligand Atoms
1	166A	GLU	5.01		Sulfonium	4735

DMS-A-813

Interacting chains: A

Figure 1a. ROCCUFFIRNATM_2Z9K_binding site(s) in 2Z9K (3c-like proteinase).DMS-A-803

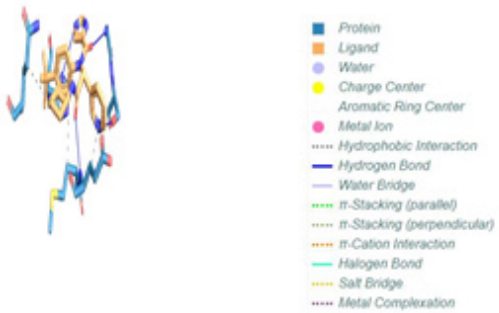

Index	Residue	AA	Distance	Ligand Atom	Protein Atom
1	41A	HIS	3.75	4670	609
2	165A	MET	3.90	4673	2529
3	166A	GLU	3.86	4661	2546
4	189A	GLN	3.90	4657	2881

Index	Residue	AA	Distance H-A	Distance D-A	Donor Angle	Protein donor?	Sidechain	Donor Atom	Acceptor Atom
1	41A	HIS	3.46	3.79	106.13			611 [Npl]	4680 [N2]
2	143A	GLY	2.17	2.94	148.03			2216 [Nam]	4682 [O2]
3	144A	SER	3.14	3.42	101.78			2228 [O3]	4679 [N2]
4	166A	GLU	1.98	2.80	158.32			2542 [Nam]	4683 [O2]

```
Interacting chain(s): A


**Hydrogen Bonds**


+-------+---------+----------+-----------+-------------+--------------+-----------+----------+----------+-----------+-----------+----------+-----------+------------+--------------+----
---------------------+------- -------------------+


| RESNR | RESTYPE | RESCHAIN | RESNR_LIG | RESTYPE_LIG | RESCHAIN_LIG | SIDECHAIN | DIST_H-A | DIST_D-A | DON_ANGLE | PROTISDON
| DONORIDX |


DONORTYPE | ACCEPTORIDX | ACCEPTORTYPE | LIGCOO           | PROTCOO


+=======+=========+==========+===========+=============+==========


====+===========+==========+==========+===========+===========+===


=======+===========+=============+==============+=================


========+==========================+
| 144  | SER       | A           | 803        | DMS       | A           | True| 3.66              | 3.99       | 102.68    |
True   | 1114       | O3          | 4736       | O2          | 35.403, -33.742, -8.029 | 37.550, -32.180, -
11.001 |
+-------              +---------    +----------   +----------- +-------------              +--------------             +----------- +----------   +----------   +-
----------              +----------- +----------   +----------- +-------------              +--------------             +------------------------ +-------
-------------------    +
**Salt Bridges**
+        -------+---------           +----------   +             -----------+ -------------+              --------------+------       +             -----------+ -----------+----
----------              +-------------------------                   +------------------------- +
| RESNR | RESTYPE | RESCHAIN | RESNR_LIG | RESTYPE_LIG | RESCHAIN_LIG |
DIST | PROTISPOS | LIG_GROUP | LIG_IDX_LIST | LIGCOO | PROTCOO
|
+=======+=========+==========+===========+=============+==========


====+======+===========+===========+==============+===============


==========+=========================+
|166 |GLU |A       | 803        | DMS       | A           | 5.01 | False | Sulfonium | 4735
| 36.185, -32.686, -7.387 | 36.922, -36.568, -4.314 |


+-------+---------+----------+-----------+-------------+--------------+------+-----------+-----------+---- ----------+------------------------+------------------------+
DMS:A:813 (DMS) - SMALLMOLECULE


-------------------------------


Interacting chain(s): A
```

Water Bridges

+-------+---------+----------+----------+-----------+-----------+---------+---------+----------+-----------+----------+----------+----------+-----------+-----------+----------+---------+-----------------+---------+-----------------------+-----------------------+

| RESNR | RESTYPE | RESCHAIN | RESNR_LIG | RESTYPE_LIG | RESCHAIN_LIG |

DIST_A-W | DIST_D-W | DON_ANGLE | WATER_ANGLE | PROTISDON |

DONOR_IDX | DONORTYPE | ACCEPTOR_IDX | ACCEPTORTYPE | WATER_IDX |

LIGCOO | PROTCOO | WATERCOO |

+=======+=========+==========+===========+=============+==========

====+==========+==========+===========+=============+===========+=

==========+===========+==============+==============+===========+=

==========================+==========================+=============

==========+

| 6 | MET | A | 813 | DMS | A | 3.97 | 2.93 | 129.48 | 78.97 |

True | 42 | Nam | 4740 | O2 | 4799 | 34.670, -48.022, -27.925 |

38.814, -48.573, -24.111 | 35.895, -48.790, -24.226 |

+------- +--------- +--------- +---------- +----------- + ----------- +---------- +---------- +---------- +-

---------- +---------- +---------- +---------- +----------- +----------- +---------- +----------

--------- +------------------------ +------------------------+

Salt Bridges

+-------+---------+----------+----------+-----------+-----------+------+----------+----------+---- ---------+------------------------+------------------------+

| RESNR | RESTYPE | RESCHAIN | RESNR_LIG | RESTYPE_LIG | RESCHAIN_LIG |

DIST | PROTISPOS | LIG_GROUP | LIG_IDX_LIST | LIGCOO | PROTCOO

|

+=======+=========+==========+===========+=============+==========

====+======+===========+===========+==============+===============

===========+==========================+

| 295 | ASP | A | 813 | DMS | A | | 5.38 | False | | Sulfonium | 4739 | 35.134, -46.698, -27.502 | 30.989, -48.448, -24.558 |

+------+---------+---------+---------+---------+---------+------+-------+---------+-----+---------+---------+---------+---------+---------+

pi-Cation Interactions

+------+---------+---------+---------+---------+---------+------+-------+---------+-----+---------+---------+---------+---------+

| RESNR | RESTYPE | RESCHAIN | RESNR_LIG | RESTYPE_LIG | RESCHAIN_LIG | DIST | OFFSET | PROTCHARGED | LIG_GROUP | LIG_IDX_LIST | LIGCOO | PROTCOO |

+=======+=========+=========+=========+=========+=========+=====+=======+=========+=====+=========+=========+=========+=========+

| 8 | PHE | A | 813 | DMS | A | | 4.40 | 0.66 | False | sulfonium | 4739 | 35.134, -46.698, -27.502 | 33.201, -42.800, -28.140 |

+------+---------+---------+---------+---------+---------+------+-------+---------+-----+---------+---------+---------+---------+---------+

DMS:B:802 (DMS) - SMALLMOLECULE

Interacting chain(s): B

Salt Bridges

+------+---------+---------+---------+---------+---------+------+---------+---------+---------+---------+---------+---------+

| RESNR | RESTYPE | RESCHAIN | RESNR_LIG | RESTYPE_LIG | DIST | PROTISPOS | LIG_GROUP | LIG_IDX_LIST | LIGCOO | RESCHAIN_LIG | | PROTCOO

+=======+=========+==========+===========+=============+==========

====+======+===========+===========+==============+===============

===========+==========================+

| 166 | GLU | B | 802 | DMS | B | 4.89 | False | Sulfonium | 4748

| 47.864, -56.126, -36.130 | 46.893, -59.847, -33.114 |

+------ +-------- +--------- +---------- +---------- +---------- + ------+ ----------+ ----------+----

---------- +---------- +----------+

DMS:B:812 (DMS) - SMALLMOLECULE

Interacting chain(s): B

Hydrogen Bonds

+-------+---------+---------+----------+----------+----------+---------+---------+----------+----------+---------+----------+----------+----------+----
----------+------ ----------+

| RESNR | RESTYPE | RESCHAIN | RESNR_LIG | RESTYPE_LIG | RESCHAIN_LIG | SIDECHAIN | DIST_H-A | DIST_D-A | DON_ANGLE | PROTISDON
| DONORIDX |

DONORTYPE | ACCEPTORIDX | ACCEPTORTYPE | LIGCOO | PROTCOO

|

+=======+=========+==========+===========+=============+==========

====+===========+==========+==========+==========+==========+===

=======+===========+=============+==============+=================

=========+==========================+

| 298 | ARG | B | 812| DMS | B | True| 1.99 | 2.85 | 144.34 |

True | 4672 | Ng+ | 4753 | O2 | 48.111, -39.487, -16.305 | 50.942, -39.249,

-16.558 |

+-------+---------+---------+----------+----------+----------+---------+---------+----------+----------+---------+----------+----------+----------+----
----------+------ ----------+

```
**Water Bridges**

+-------+---------+----------+-----------+-------------+--------------+----------+----------+-----------+-------------+-----------+-----------+-----------+-------------+--------------
+-----------+----------------- ---------+-------------------------+-------------------------+

| RESNR | RESTYPE | RESCHAIN | RESNR_LIG | RESTYPE_LIG | RESCHAIN_LIG |

DIST_A-W | DIST_D-W | DON_ANGLE | WATER_ANGLE | PROTISDON |

DONOR_IDX | DONORTYPE | ACCEPTOR_IDX | ACCEPTORTYPE | WATER_IDX |

LIGCOO           | PROTCOO           | WATERCOO          |

+=======+=========+==========+===========+=============+==========

====+==========+==========+===========+============+===========+=

==========+===========+=============+=============+===========+=

========================+==========================+=============

=============+

| 6      | MET      | B          | 812       | DMS      | B          | 4.03      | 3.27      | 115.07    | 79.20      |
True   | 2404                  | Nam      | 4753     | O2        | 5163      | 48.111, -39.487, -16.305 |
44.043, -43.542, -17.221 | 47.204, -43.417, -16.402 |
+-------             +---------    +----------   +----------- +-------------            +            --------------            +----------   +----------   +----------- +-
------------         +----------- +----------- +----------- +--------------           +--------------           +----------- +-----------------
---------            +-------------------------               +-------------------------+

**pi-Cation Interactions**

+-------+---------+----------+-----------+-------------+--------------+------+--------+------------+----- ------+-------------+------------------------+-------------------------+


| RESNR | RESTYPE | RESCHAIN | RESNR_LIG | RESTYPE_LIG | RESCHAIN_LIG | DIST | OFFSET | PROTCHARGED | LIG_GROUP | LIG_IDX_
LIST | LIGCOO PROTCOO |

|

+=======+=========+==========+===========+============+==========

====+======+========+=============+==========+=============+====

======================+==========================+
```

| 8 |PHE |B | 812 | DMS | B | 4.36 | 0.95 | False | sulfonium |
4752 | 48.108, -39.567, -17.768 | 50.199, -37.954, -21.238 |

+-------+---------+----------+----------+----------+----------+------+-------+---------+----- ------+----------+----------+----------

DOZ:A:901 (DOZ) - SMALLMOLECULE

Interacting chain(s): A

Hydrogen Bonds

+-------+---------+----------+----------+----------+----------+----------+----------+----------+----------+----------+----------+----------+----------+----
----------+------- ----------+

| RESNR | RESTYPE | RESCHAIN | RESNR_LIG | RESTYPE_LIG | RESCHAIN_LIG | SIDECHAIN | DIST_H-A | DIST_D-A | DON_ANGLE | PROTISDON
| DONORIDX |

DONORTYPE | ACCEPTORIDX | ACCEPTORTYPE | LIGCOO | PROTCOO

|

+=======+=========+==========+==========+==========+==========

====+==========+==========+==========+==========+==========+===

=======+==========+==========+==========+==========

========+==========+

| 164 | HIS | A | 901 | DOZ | A | False | 2.95 | 3.73 | 138.78 |
False | 4745 | O3 | 1266 | O2 | 33.183, -27.630, -6.449 | 31.059, -30.039, -
8.348 |
+------- +--------- +--------- +---------- +---------- +---------- +---------- + ---------- +---------- +-
--------- +---------- +--------- +---------- +---------- +---------- +---------- +-------
---------- +

Water Bridges

+-------+---------+----------+----------+----------+----------+----------+----------+----------+----------+----------+----------+----------+----------
+----------+---------- -------+----------+----------+

| RESNR | RESTYPE | RESCHAIN | RESNR_LIG | RESTYPE_LIG | RESCHAIN_LIG | DIST_A-W | DIST_D-W | DON_ANGLE | WATER_ANGLE |

PROTISDON |

DONOR_IDX | DONORTYPE | ACCEPTOR_IDX | ACCEPTORTYPE | WATER_IDX |

LIGCOO | PROTCOO | WATERCOO |

+=======+=========+==========+===========+=============+==========

====+==========+==========+===========+=============+===========+=

==========+===========+==============+==============+===========+=

=======================+========================+===============

==========+

| 25 | THR | A | 901 | DOZ | A | 3.52 | 4.01 | 104.45 | 71.67 |
True | 178 | O3 | 4744 | N3 | 5120| 34.346, -25.155, -7.918 | 35.074,
-19.395, -6.573 | 33.928, -22.975, -5.184 |
+------- +--------- +--------- +---------- +---------- +---------- +---------- +---------- +-
---------- +---------- +---------- +---------- +---------- +---------- +----------
------- +---------- +---------- +

Metal Complexes

+-------+---------+---------+----------+----------+----------+----------+---------- -+----------+----------+------+----------+-------+----------
-------+----------+------- ----------+----------+

| RESNR | RESTYPE | RESCHAIN | RESNR_LIG | RESTYPE_LIG | RESCHAIN_LIG | METAL_IDX | METAL_TYPE | TARGET_IDX | TARGET_TYPE |
COORDINATION |

DIST | LOCATION | RMS | GEOMETRY | COMPLEXNUM | METALCOO

| TARGETCOO |

+=======+=========+==========+===========+=============+==========

====+===========+============+============+=============+=========

=====+======+===================+=======+===================+====

========+=========================+=========================+

| 41 | HIS | A | 901 | DOZ | A | 4743 | Zn | 312 | N |
3 | 2.12 | protein.sidechain | 27.36 | trigonal.pyramidal | 1 | 33.603, -26.958, -

8.187 | 31.690, -26.097, -8.509 |

+------- +--------- +---------- +---------- +---------- +---------- +---------- +----------+----------
-+---------- +---------- +------ +---------- +------- +---------- +----------+-------
---------- +---------- +

| 145 | CYS | A | 901 | DOZ | A | 4743 | Zn | 1120 | S
| 3 | 2.28 | protein.sidechain | 27.36 | trigonal.pyramidal | 1 | 33.603, -26.958, -
8.187 | 34.122, -28.774, -9.460 |

+------- +--------- +---------- +---------- +---------- +---------- + ---------- +----------+----------
-+---------- +---------- +------ +---------- +------- +---------- +----------+-------
---------- +---------- +

| 901 | DOZ | A | 901 | DOZ | A | 4743 | Zn | 4744 | N
| 3 | 1.97 | ligand | 27.36 | trigonal.pyramidal | 1 | 33.603, -26.958, -8.187 |
34.346, -25.155, -7.918 |

+------- +--------- +---------- +---------- +---------- +---------- + ---------- +----------+----------
-+---------- +---------- +------ +---------- +------- +---------- +----------+-------
---------- +---------- +

DOZ:B:902 (DOZ) - SMALLMOLECULE

Interacting chain(s): B

Metal Complexes

+-------+---------+---------+----------+----------+----------+----------+---------- -+----------+----------+------+----------+-------+----------
--------+----------+------- ----------+----------+

| RESNR | RESTYPE | RESCHAIN | RESNR_LIG | RESTYPE_LIG | RESCHAIN_LIG | METAL_IDX | METAL_TYPE | TARGET_IDX | TARGET_TYPE |
COORDINATION |

DIST | LOCATION | RMS | GEOMETRY | COMPLEXNUM | METALCOO | TARGETCOO |

+=======+=========+==========+==========+==========+==========

====+==========+==========+==========+==========+=========

=====+======+==========+=======+==========+====

========+==========+==========+
| 41 | HIS | B | 902 | DOZ | B | 4756| Zn | 2674 | N |
3 | 2.10 | protein.sidechain | 10.64 | trigonal.pyramidal | 1 | 51.015, -53.952, -
41.217 | 52.956, -53.584, -41.918 |

+------- +--------- + ---------+---------- + ----------+---------- +---------- +----------+----------
-+---------- +---------- +------ +---------- +------- +---------- +----------+-------
---------- +---------- +

```
| 145  | CYS      | B          | 902       | DOZ      | B          | 4756      | Zn        | 3482      | S
| 3      | 2.29 | protein.sidechain | 10.64 | trigonal.pyramidal | 1                          | 51.015, -53.952, -
41.217 | 50.319, -53.103, -39.204 |
+-------              +---------   +----------  +-----------  +-------------            +--------------            +-----------  +------------+-----------
-+-------------       +--------------           +------       +-------------------      +-------      +-------------------       +------------+-------
-------------------   +---------------------------+
| 902  | DOZ      | B          | 902       | DOZ      | B          | 4756      | Zn        | 4757      | N
| 3      | 1.97 | ligand                    | 10.64 | trigonal.pyramidal | 1   | 51.015, -53.952, -41.217 |
50.774, -55.886, -40.954 |
+-------              +---------   +----------  +-----------  +-------------            +--------------            +-----------  +------------+-----------
-+-------------       +--------------           +------       +-------------------      +-------      +-------------------       +------------+-------
-------------------   +---------------------------+
```

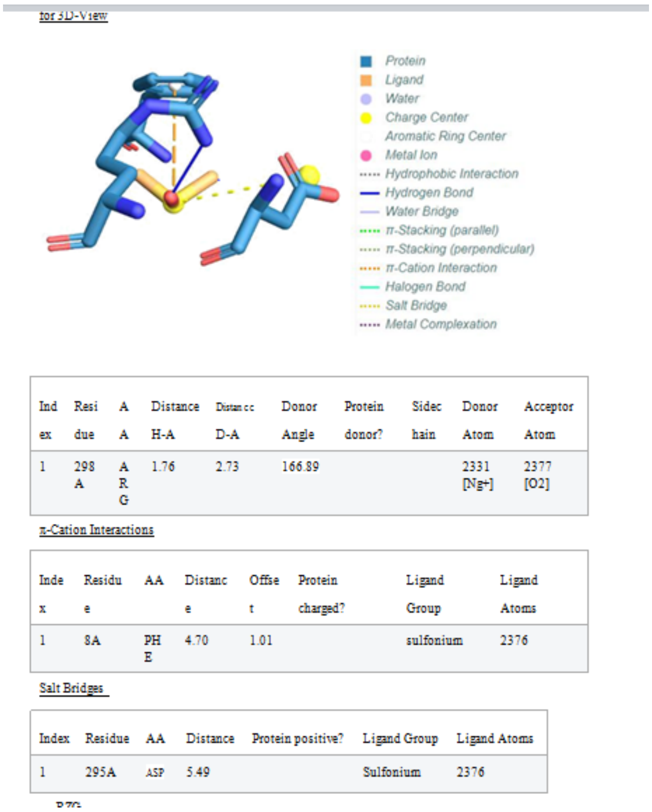

Index	Residue	AA	Distance H-A	Distance D-A	Donor Angle	Protein donor?	Sidechain	Donor Atom	Acceptor Atom
1	298A	ARG	1.76	2.73	166.89			2331 [Ng+]	2377 [O2]

π-Cation Interactions

Index	Residue	AA	Distance	Offset	Protein charged?	Ligand Group	Ligand Atoms
1	8A	PHE	4.70	1.01		sulfonium	2376

Salt Bridges

Index	Residue	AA	Distance	Protein positive?	Ligand Group	Ligand Atoms
1	295A	ASP	5.49		Sulfonium	2376

Figure 2a. RoccuffirnaTM_6W63_ binding site(s) in 6W63, X77-A-401. | 902 | DOZ | B | 902 | DOZ | B | 4756 | Zn | 4757 | N

Prediction of noncovalent interactions for PDB structure 6W63

==

Created on 2020/11/03 using PLIP v1.4.4

If you are using PLIP in your work, please cite:

Salentin,S. et al. PLIP: fully automated protein-ligand interaction profiler.

Nucl. Acids Res. (1 July 2015) 43 (W1): W443-W447. doi: 10.1093/nar/gkv315

X77:A:401 (X77) - SMALLMOLECULE

Interacting chain(s): A

Hydrophobic Interactions

+-------+---------+---------+----------+----------+----------+-----+----------+---------- -+----------+----------+

| RESNR | RESTYPE | RESCHAIN | RESNR_LIG | RESTYPE_LIG | DIST | LIGCARBONIDX | PROTCARBONIDX | LIGCOO |

RESCHAIN_LIG |

| PROTCOO

+=======+=========+==========+==========+==========+==========

====+======+==========+==========+==========

===+==========+

| 41 | HIS | A | 401 | X77 | A | 3.75 | 4670 | 609 | -20.444,

13.613, -29.034 | -19.778, 13.574, -32.721 |

+------- +--------- +--------- +---------- +---------- +---------- +------ +---------- +----------

-+---------- +----------+

| 165 | MET | A | 401 | X77 | A | 3.90 | 4673 | 2529 | -

19.389, 17.775, -28.688 | -16.611, 16.152, -26.489 |

+------- +--------- +--------- +---------- +---------- +---------- +------ +---------- +----------

-+---------- +----------+

| 166 | GLU | A | 401 | X77 | A | 3.86 | 4661 | 2546 | -

17.350, 23.138, -25.438 | -16.439, 20.244, -23.055 |

+------- +--------- +--------- +---------- +---------- +---------- +------ +---------- +----------

-+---------- +----------+

| 189 | GLN | A | 401 | X77 | A | 3.90 | 4657 | 2881 | -

21.763, 15.894, -23.429 | -24.934, 13.635, -23.312 |

+------- +--------- +--------- +---------- +---------- +---------- +------ +---------- +----------

-+---------- +----------+

Hydrogen Bonds

+-------+---------+---------+----------+----------+----------+----------+---------+---------+----------+----------+---------+----------+----------+----------+----

----------+------ ----------+

| RESNR | RESTYPE | RESCHAIN | RESNR_LIG | RESTYPE_LIG | RESCHAIN_LIG | SIDECHAIN | DIST_H-A | DIST_D-A | DON_ANGLE | PROTISDON | DONORIDX |

DONORTYPE | ACCEPTORIDX | ACCEPTORTYPE | LIGCOO |

| PROTCOO

+=======+=========+==========+===========+=============+==========

====+===========+==========+==========+===========+===========+===

=======+===========+=============+==============+=================

=========+==========================+

| 41 |HIS |A | 401 | X77 | A | True | 3.46 | 3.79 | 106.13 |

True | 611 | Npl | 4680 | N2 | -20.860, 19.573, -32.520 | -19.394, 16.086, -

32.767 |

+------- +--------- +--------- + ---------- +------------ +------------ +---------- +---------- +---------- +-

--------- +---------- +--------- +---------- +------------ +------------ +-----------------------+------

---------- +

| 143 | GLY | A | 401 | X77 | A | False | 2.17 | 2.94 | 148.03 |

True | 2216 | Nam | 4682 | O2 | -19.635, 22.244, -29.036 | -18.779, 24.455,

-30.773 |

+------- +--------- +--------- + ---------- +------------ +------------ +---------- +---------- +---------- +-

--------- +---------- +--------- +---------- +------------ +------------ +-----------------------+------

---------- +

| 144 | SER | A | 401 | X77 | A | True | 3.14 | 3.42 | 101.78 |

True | 2228 | O3 | 4679 | N2 | -16.096, 21.679, -26.816 | -14.503, 23.707,

-29.056 |

+------- +--------- +--------- + ---------- +------------ +------------ +---------- +---------- +---------- +-

--------- +---------- +--------- +---------- +------------ +------------ +-----------------------+------

---------- +

| 166 | GLU | A | 401 | X77 | A | False | 1.98 | 2.80 | 158.32 |

True | 2542 | Nam | 4683 | O2 | -18.546, 18.654, -26.028 | -16.172, 18.348,

-24.583 |

+------- +--------- +--------- + ---------- +------------ +------------ +---------- +---------- +---------- +-

--------- +---------- +--------- +---------- +------------ +------------ +-----------------------+------

Figure 2b. RoccuffirnaTM_6W63_ binding site(s) in 6W63, DMS-A-402 Click for 3D-View.

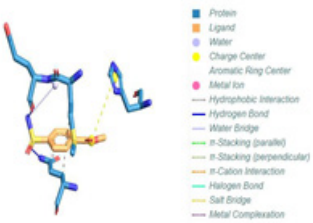

Hydrophobic Interactions

Index	Residue	AA	Distance	Ligand Atom	Protein Atom
1	165A	MET	3.96	2384	1284
2	189A	GLN	3.68	2389	1469
3	189A	GLN	3.75	2388	1468

Water Bridges

Index	Residue	AA	Dist. A-W	Dist. D-W	Donor Angle	Water Angle	Protein donor?	Donor Atom	Acceptor Atom	Water Atom
1	166A	GLU	4.01	2.87	172.42	89.78		1288 [Nam]	2392 [N3]	2573

Salt Bridges

Index	Residue	AA	Distance	Protein positive?	Ligand Group	Ligand Atoms
1	41A	HIS	5.18		Carboxylate	2393, 2394

Hydrogen Bonds

Index	Residue	AA	Distance H-A	Distance D-A	Donor Angle	Protein donor?	Sidechain	Donor Atom	Acceptor Atom
1	166A	GLU	2.01	2.99	161.20			2392 [N3]	1291 [O2]
2	189A	GLN	3.08	3.67	120.00	✔	✔	1472 [Nam]	2396 [O2]

Prediction of noncovalent interactions for PDB structure 5R80

==========

Created on 2020/11/03 using PLIP v1.4.4

If you are using PLIP in your work, please cite:

Salentin,S. et al. PLIP: fully automated protein-ligand interaction profiler.

Nucl. Acids Res. (1 July 2015) 43 (W1): W443-W447. doi: 10.1093/nar/gkv315

DMS:A:401 (DMS) - SMALLMOLECULE

Interacting chain(s):

detected.

DMS:A:402 (DMS) - SMALLMOLECULE

```
-------------------------------

Interacting chain(s): A

 **Hydrogen Bonds**


+-------+---------+----------+-----------+-------------+--------------+-----------+----------+----------+-----------+-----------+-----
-----+-----------+-------------+--------------+----------------------+--------- --------------+


| RESNR | RESTYPE | RESCHAIN | RESNR_LIG | RESTYPE_LIG | RESCHAIN_LIG | SIDECHAIN | DIST_H-A |
DIST_D-A | DON_ANGLE | PROTISDON | DONORIDX |


DONORTYPE | ACCEPTORIDX | ACCEPTORTYPE | LIGCOO           | PROTCOO

+=======+=========+==========+===========+=============+==========

====+===========+==========+==========+===========+===========+===

=======+===========+=============+==============+=================

======+========================+

| 298     | ARG   | A        | 402| DMS       | A        | True| 1.76        | 2.73     | 166.89|

True      | 2331    | Ng+    | 2377    | O2       | 6.971, -0.756, -7.541 | 9.700, -0.883, -

7.581 |

+------- +---------           +----------          +-----------        +-------------      +--------------     +-----------         +----------
+----------           +-

----------            +-----------        +----------          +-----------        +-------------      +--------------     +----------------------
+---------

--------------       +

**Salt Bridges**

+-------+---------+----------+-----------+-------------+--------------+------+-----------+-----------+---- ----------+-----------------
------+----------------------+

| RESNR | RESTYPE | RESCHAIN | RESNR_LIG | RESTYPE_LIG | RESCHAIN_LIG | DIST | PROTISPOS | LIG_
GROUP | LIG_IDX_LIST | LIGCOO | PROTCOO |

+=======+=========+==========+===========+=============+==========

====+======+===========+===========+=============+===============

========+========================+

| 295     | ASP    | A        | 402      | DMS   | A                   | 5.49 | False                 | Sulfonium | 2376

| 6.081, -1.005, -6.367 | 10.436, 2.231, -5.560 |

+------- +---------           +----------          +-----------        +-------------      +--------------     +------   +          -----------+
-----------+----
```

---------- +---------- +---------- +

pi-Cation Interactions

+-------+---------+----------+----------+----------+----------+------+--------+----------+----- ------+----------+----------+----------+

| RESNR | RESTYPE | RESCHAIN | RESNR_LIG | RESTYPE_LIG | RESCHAIN_LIG | DIST | OFFSET | PROTCHARGED | LIG_GROUP | LIG_IDX_LIST | LIGCOO PROTCOO |

|

+=======+=========+==========+==========+==========+==========

====+======+========+==========+==========+==========+====

==========+==========+

| 8 |PHE |A| 402 | DMS | A | 4.70 | 1.01 | False | sulfonium |

2376 | 6.081, -1.005, -6.367 | 8.339, -4.556, -4.264 |

+------- + ---------+ ----------+ ----------+---------- + ----------+------ +--------+ ----------+-----

------ +---------- +---------- +----------

DMS:A:403 (DMS) - SMALLMOLECULE

Interacting chain(s):

detected.

RZG:A:404 (RZG) - SMALLMOLECULE

Interacting chain(s): A

Hydrophobic Interactions

+-------+---------+----------+----------+----------+----------+------+----------+---------- -+----------+-----------+

| RESNR | RESTYPE | RESCHAIN | RESNR_LIG | RESTYPE_LIG | RESCHAIN_LIG | DIST | LIGCARBONIDX | PROTCARBONIDX | LIGCOO | PROTCOO

|

+=======+=========+==========+==========+==========+==========

====+======+==========+==========+==========

+==========+

| 165 | MET | A | 404 | RZG | A | 3.96 | 2384 | 1284 |

13.459, 2.162, 22.819 | 12.458, 1.105, 19.137 |

+------- +--------- +---------- +---------- +---------- + ----------+------ +----------

--- +----------

-+---------- +---------- +

| 189 | GLN | A | 404 | RZG | A | 3.68 | 2389 | 1469 | 11.044,

2.322, 24.179 | 12.243, 3.597, 27.411 |

+------- +--------- +---------- +---------- +---------- + ----------+------ +----------
--- +----------

-+---------- +---------- +

| 189 | GLN | A | 404 | RZG | A | 3.75 | 2388 | 1468 | 11.707,

1.106, 24.084 | 13.298, 2.520, 27.177 |

+------- +--------- +---------- +---------- +---------- + ----------+------ +----------
--- +----------

-+---------- +---------- +

Hydrogen Bonds

+-------+---------+----------+----------+----------+----------+----------+----------+----------+----------+----------+-----
-----+----------+----------+----------+----------+--------- ----------+

| RESNR | RESTYPE | RESCHAIN | RESNR_LIG | RESTYPE_LIG | RESCHAIN_LIG | SIDECHAIN | DIST_H-A | DIST_D-A | DON_ANGLE | PROTISDON | DONORIDX |

DONORTYPE | ACCEPTORIDX | ACCEPTORTYPE | LIGCOO | PROTCOO

|

+=======+=========+==========+==========+==========+==========

====+==========+==========+==========+==========+==========+===

=======+==========+==========+==========+==========

======+=========================+

| 166 | GLU | A | 404 | RZG | A | False | 2.01 | 2.99 | 161.20|

False | 2392 | N3 | 1291 | O2 | 9.311, 5.041, 22.782 | 10.444, 4.777,

20.029 |

+------- +--------- +---------- +---------- +---------- +---------- +---------- +----------
+---------- +-

---------- +---------- +---------- +---------- +---------- +---------- +----------
+---------

---------- +

| 189 | GLN | A | 404| RZG | A | True| 3.08 | 3.67 | 120.00|

True | 1472 | Nam | 2396 | O2 | 10.485, 5.379, 25.107 | 10.139, 4.011,

28.500 |

+------- +--------- +---------- +---------- +---------- +---------- +---------- +----------
+---------- +-

---------- +---------- +---------- +---------- +---------- +---------- +---------- +---------

---------- +

Water Bridges

+-------+---------+----------+----------+----------+----------+----------+----------+----------+----------+----------+----------+----------+----------+----------+----------+----------+----------+

| RESNR | RESTYPE | RESCHAIN | RESNR_LIG | RESTYPE_LIG | RESCHAIN_LIG |

DIST_A-W | DIST_D-W | DON_ANGLE | WATER_ANGLE | PROTISDON |

DONOR_IDX | DONORTYPE | ACCEPTOR_IDX | ACCEPTORTYPE | WATER_IDX |

LIGCOO | PROTCOO | WATERCOO |

+=======+=========+==========+==========+==========+==========

====+==========+==========+==========+==========+==========+=

==========+==========+==========+==========+==========+=

==========+==========+==========+

| 166 | GLU | A | 404 | RZG | A | 4.01 | 2.87 | 172.42 | 89.78

| True | 1288 | Nam | 2392 | N3 | 2573| 9.311, 5.041, 22.782 | 9.967,

2.685, 18.385 | 9.274, 1.499, 20.904 |

+------- +--------- +---------- +---------- +---------- + ----------+ ---------- +---------- + ----------+-

---------- +---------- +---------- +---------- +---------- +---------- +---------- +----------

-----+---------- +---------- +

Salt Bridges

+-------+---------+----------+----------+----------+----------+------+----------+----------+-- ----------+----------+----------+

| RESNR | RESTYPE | RESCHAIN | RESNR_LIG | RESTYPE_LIG | RESCHAIN_LIG |

DIST | PROTISPOS | LIG_GROUP | LIG_IDX_LIST | LIGCOO | PROTCOO

|

+=======+=========+==========+==========+==========+==========

====+======+==========+==========+==========+==========

==========+==========+

| 41 | HIS | A | 404 | RZG | A | 5.18 | True | Carboxylate |

2393,2394 | 13.944, -0.877, 23.349 | 11.774, -4.812, 20.770 |

+------- +--------- + ----------+ ----------+ ----------+ ----------+------ + ----------+---------- +--

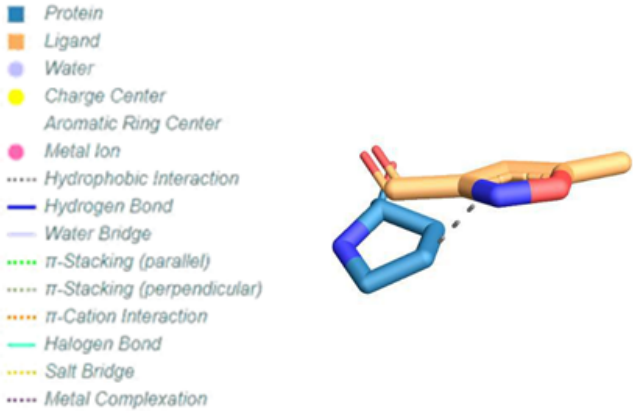

in PyMol (.pse) format | *as (.png) image*

Hydrophobic Interactions

Index	Residue	AA	Distance	Ligand Atom	Protein Atom
1	168A	PRO	3.53	2369	1303

PJE (composite ligand)

PJE-C-5 Composite ligand consists of PJE:C:5, 010:C:6.

Figure 2c. RoccuffirnaTM_6LU7_2 binding site(s) in 6LU7. 02J-C-1.

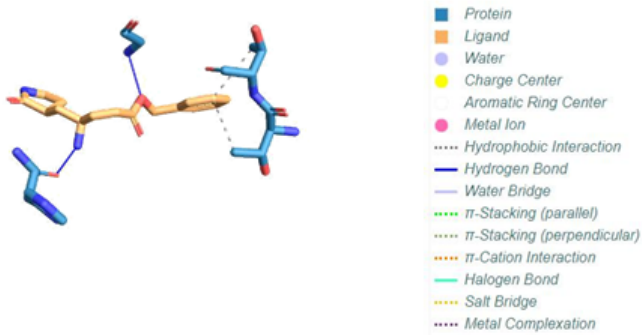

Index Residue AA Distance Ligand Atom Protein Atom

Index	Residue	AA	Distance	Ligand Atom	Protein Atom
1	25A	THR	3.73	2415	179
2	26A	THR	3.81	2415	186

Hydrogen Bonds

Index	Residue	AA	Distance H-A	Distance D-A	Donor Angle	Protein donor?	Sidechain	Donor Atom	Acceptor Atom
1	143 A	GLY	1.93	2.80	145.29			1105 [Nam]	2411 [O3]
2	164 A	HIS	2.16	3.07	153.73	✖	✖	2408 [N3]	1266 [O2]

Figure 2d. RoccuffirnaTM_6LU7_2 binding site(s) in 6LU7 PJE-C-5.

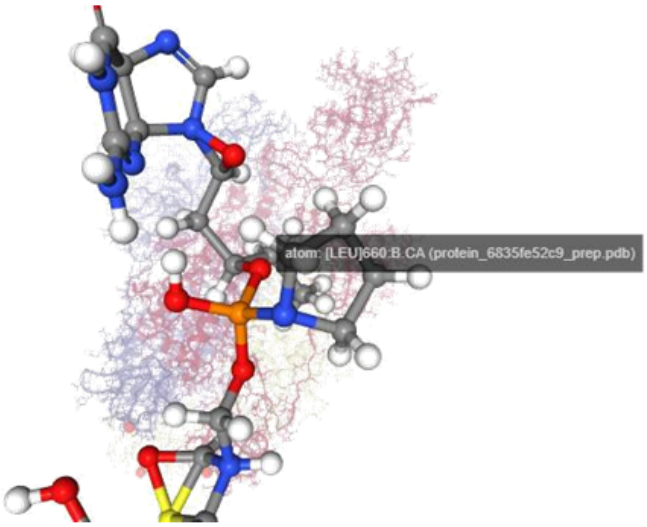

File	Model	T.Energy	I.Energy	vdW	Coul	NumRotors	RMSD	Score
ligand_ac3a22_1_run_20.log	1	-84.576	-0.705	-0.000	-0.705	12	0.000	16.203
ligand_ac3a22_1_run_20.log	6	-84.575	-0.704	-0.000	-0.704	12	8.613	16.203
ligand_ac3a22_1_run_20.log	2	-84.575	-0.704	-0.000	-0.704	12	8.286	16.203

Figure 3a. Contact residues of the Roccuffirna chemical strucuture when docked onto the SARS-COV-2 protein binding sites of the (pdb:6xs6) protein targets. Electrostatic surface view of active site pocket of the (pdb:6xs6) protein targets bound to the Roccuffirna small molecule

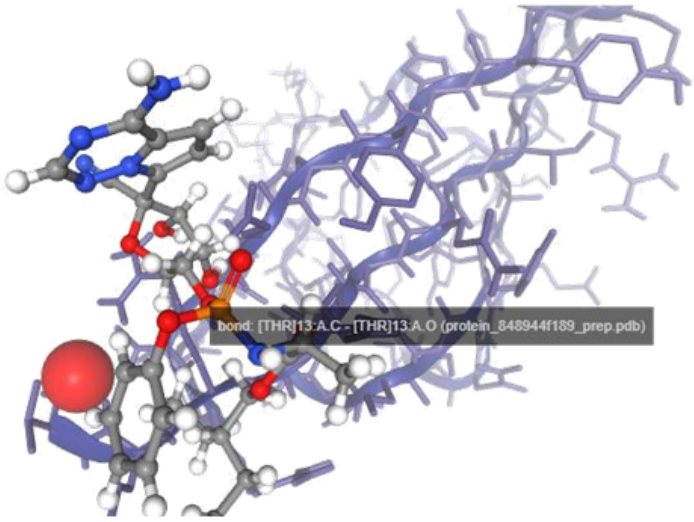

File	Model	T.Energy	I.Energy	vdW	Coul	NumRotors	RMSD	Score
ligand_f926363931_1_run_20.log	1	23.905	-26.781	1.900	-28.681	14	0.000	-5.987
ligand_f926363931_1_run_9.log	1	24.268	-28.081	-2.302	-25.779	14	4.230	-6.488
ligand_f926363931_1_run_16.log	2	24.641	-26.765	2.068	-28.833	14	2.625	-6.089

Figure 3b. Contact residues of the Remdesivir drug when docked onto the SARS-COV-2 protein binding sites of the (pdb:1xak) protein targets. Electrostatic surface view of active site pocket of the (pdb:1xak) protein targets bound to the Remdesivir small molecule.

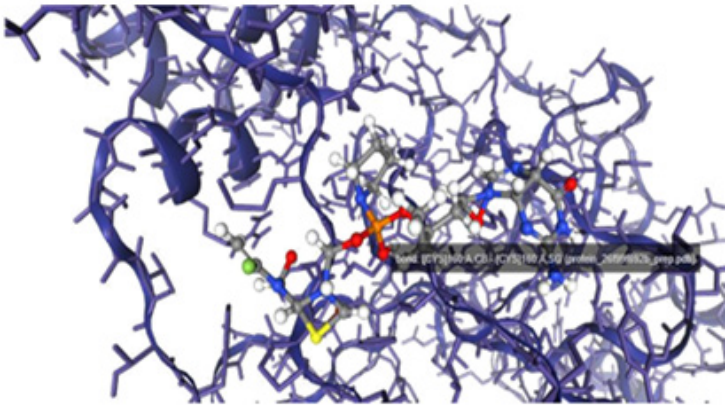

File	Model	T.Energy	I.Energy	vdW	Coul			
NumRotors	RMSD	Score						
ligand_7ce85cbfb3_1_run_7.log	1	-116.717	-36.220	-13.116	-23.104			
12	0.000	-7.447						
ligand_7ce85cbfb3_1_run_14.log	1	-115.525	-33.962	-9.287	-24.675			
12	7.077	-7.010						
ligand_7ce85cbfb3_1_run_3.log	2	-115.230	-33.212	-12.097	-21.115			
12	3.617	-7.169						

Figure 3c. Contact residues of the Roccuffirna chemical strucuture when docked onto the SARS-COV-2 protein binding sites of the (pdb:6yb7) protein targets. Electrostatic surface view of active site pocket of the (pdb:6yb7) protein targets bound to the Roccuffirna small molecule.

Discussions

In this project, considering a spacetime containing a degenerate horizon containing a degenerate horizon with a compact cross section H and assume the dominant energy condition holds. If ≥ 0 then H S2, or the induced metric on the horizon is Ricci flat. If <0 and (H) < 0 except for the special case where the near-horizon geometry is flat (so = 0) and H T2. If < 0 and (H)<0 the area of H satisfies AH ≥ 2π−1(H) with equality if and only if the near-horizon geometry is AdS2 × g, where g is a compact quotient of hyperbolic space of genus D(p,q)=(p1−q1)2+(p2−q2)2++(pn−qn)2 Average Accuracy=∑i=1lTPi+TNiTPi+FNi+FPi+TNi/l kappa=P(A)−P(E)1−P(E) kappa =P(A)−P(E)1−P(E)=0.9−0.44041−0.4404≈0.82 D(p,q)=(p1−q1)2+(p2−q2)2+ +(pn−qn)2 Average Accuracy=∑i=1lTPi+TNiTPi+FNi+FPi+TNi /l kappa=P(A)−P(E)1−P(E)kappa=P(A)−P(E)1−P(E)=0.9−0.44041−0.4404≈0.82Ri=[MACi,1RSSi,1¯MACi,2RSSi,2¯MACi,mRSSi,m¯]dsig(li,lj) =Ri,Rjp=(∑k=1m(RSSi,k−RSSj,k)p)1/p dsig−avg(li,lj)=∑k=1m(RSSi,k−RSSj,k)2/mdpos(li,lj)=(xi−xj)2+(yi−yj)2r(i,j)=s(i,j)−maxj′≠j{a(i,)+s(i,j′)}a(i,j)=min{0,r(j,j)+∑i′≠i,jmax{0,r(i′,j)}}a(j,j)=∑i′≠jmax{0,r(i′,j)}{x=∑i=1m(xi×1di)/∑i=1m1diy=∑i=1m(yi×1di)/∑i=1m1dig,cossin|xj=cos1jcosijcosmjsin1jsinijsinmj|Aj=|x1j|x2j|xmj=cos1jsin1jcos2jsin2jcosmjsinmj=cos1j×cos2j××cosmjcos1j×cos2j××sinmjsin1j×sin2j××sinmj=Aj1Aj2Aj2mxjh=Ajh+12bj−aj2mh,ijk(t+1)=c1r1Pijk(t)+c2r2Gij(t)(c1r1+c2r2)±wln[1/uijk(t)]1L∑k=1LPijk(t)−ijk(t),dq1x1dtq1=a(x2−x1)dq2x2dtq2=(c−a)x1−x1x3+cx2dq3x3dtq3=x1QFI≈∑i=01k4Re[i12]2(k2+(Brf)2)2(1Pi11+1Pi22)+(Pi11−Pi22)2Pi11+Pi22,Pijj=ijj+(−1)jiijji=(Brf)22(k2+(Brf)2)(i11−i22)−Brfk(k2+(Brf)2)Im[i12]Im[i12]i12s(0)¯sΔQFI/QFI≡QFI(Brf=0)−QFI(Brf=150nT)QFI(Brf=0) Oˆ Oˆ Δ2=Δ2Oˆ|dOˆ/d|2 Δ2Oˆ Oˆ Oˆ ¯s Oˆ=Sˆ2=(Sˆ1+Sˆ2) Here, for the first time, we generated physical and topological descriptors for finding eigenvectors and eigenvalues involved constructing (numerically) the most general five dimensional static near-horizon geometry with SO(3) rotational symmetry to construct solutions to the five-dimensional Einstein equations as applied to the Biogenetoligandorol AI-Quantum computing, entanglement complexity guidelines for (Q)SAR requirements as well as performance implications, random forest (RF), deep neural network (DNN), and gradient boosting decision tree (GBDT), to facilitate their applications to quantum chemistry and ligand based drug design methodologies. In this hybrid drug designing approach, we have merged pharmacophoric elements into the RoccuffirnaTM merged nano-structures as a system of intrinsically positioned cables filtered before evaluation and triangular bars kinematically stable to the present; (35,36,37,38,39) utilizing purely geometrical dynamics of the initial singularity and structurally valid symmetric formations of connected small molecule components, holes, [40,41,42] and voids jointed at their ends by hinged connections to form a rigid chemical scaffold with anti-COVID19 properties [1,4-22,23-43]. As a result the Roccuffirna drug design interacted at the same SARS-COV-2 protein targets of the (pdb:7bv2) with the highest negative docking values whne compared to other antiviral blockbuster FDAs and more specifically with some of 14,789 times higher to Remdesivir small molecule.

Conclusion

In summary, the main goal of this paper was to emphasize that the Roccuffirna IUPAC named = (3S,4'R,5'S)2'amino3[(2R)2{[(R){[(2R,4R)2[(1fluoroethenyl)(hydroxymethyl)amino]5oxa1lambda3thia3azabicyclo[2.1.0]pentan3yl]methoxy}(hydroxy)(pyrrolidin1

yl)phosphaniumyl]oxy}butyl]6'oxo1',4',5',6'tetrahydro2lambda6spiro[oxaziridine2,9'purin]2ylium derivatives are promising starting points for COVID19 drug discovery. By defining quantum canonical transformations algebraically in terms of a topological transformation group consisting of ordered expressions in the quantum variables q and p, consistent with the canonical commutation relations, it was possible to work outside of a specific Hilbert space and design the Roccuffirna small molecule as a source of inspiration to design and develop novel and more effective anti-SARS-COV-2 drug candidates in taking advantage of current computing technologies, to the point that it is now possible to perform reliable comparisons of numerical models with observed data. As a by-product of

the fact that the quantum canonical transformations are defined outside of the Hilbert space, they enable the construction of the Roccuffirna small molecule by applying the general solution of the wave equation, including the non-normalizable solutions as molecular modification strategies by introducing numerical cosmological calculations to investigate different quantum chemistry phenomena.

Acknowledgments

I would like to express my special thanks of gratitude to my teacher (George Grigoriadis Pharmacist) as well as our principal (Nikolaos Grigoriadis Phd Pharmacist) who gave me the golden opportunity to do this wonderful project on the Quantum Chemistry topic, which also helped me in doing a lot of Research and i came to know about so many new things I am really thankful to them.

References

1. Hui, David S. "Epidemic and Emerging Coronaviruses (Severe Acute Respiratory Syndrome and Middle East Respiratory Syndrome)." *Clin Chest Med* 38(2017): 71-86.
2. Zhu, Na, Dingyu Zhang, Wenling Wang, and Xingwang Li, et al. "A Novel Coronavirus from Patients with Pneumonia in China, 2019." *N Engl J Med* 382(2020): 727-733.
3. Paraskevis, Dimitrios, Evangelia Georgia Kostaki, Gkikas Magiorkinis, and Georgios Panayiotakopoulos, et al. "Full-Genome Evolutionary Analysis of the Novel Corona Virus (2019-nCoV) Rejects the Hypothesis of Emergence as a Result of a Recent Recombination Event." *Infect Genet Evol* 79(2020): 104212.
4. Lu, Roujian, Xiang Zhao, Juan Li, and Peihua Niu, et al. "Genomic Characterisation and Epidemiology of 2019 Novel Coronavirus: Implications for Virus Origins and Receptor Binding." *Lancet* 395(2020): 565-574.
5. Luk, Hayes KH, Xin Li, Joshua Fung, and Susanna KP Lau, et al. "Molecular Epidemiology, Evolution and Phylogeny of SARS Coronavirus." *Infect Genet Evol* 71(2019): 21-30.
6. Ziebuhr, John. "Molecular Biology of Severe Acute Respiratory Syndrome Coronavirus." *Curr Opin Mircobiol* 7(2004): 412-419.
7. Weiss, Susan R, and Julian L Leibowitz. "Coronavirus Pathogenesis." *Adv Virus Res* 81(2011): 85-164.
8. Brian DA, and RS Baric. "Coronavirus Genome Structure and Replication." *Curr Top Microbiol Immunol* 287(2005): 1-30.
9. Narayanan, Krishna, Cheng Huang, and Shinji Makino. "SARS Coronavirus Accessory Proteins." *Virus Res* 133(2008): 113-121.
10. Arndt, Ariel L, Blake J. Larson, and Brenda G. Hogue. "A Conserved Domain in the Coronavirus Membrane Protein Tail is Important for Virus Assembly." *J Virol* 84 (2010): 11418-11428.
11. Neuman, Benjamin W, Gabriella Kiss, Andreas H Kunding, and David Bhella, et al. "A Structural Analysis of M Protein in Coronavirus Assembly and Morphology." *J Struct Biol* 174(2011): 11-22.
12. Siu, Kam-Leung, Chi-Ping Chan, Kin-Hang Kok, and Patrick Chiu-Yat Woo, et al. "Suppression of Innate Antiviral Response by Severe Acute Respiratory Syndrome Coronavirus M Protein is Mediated through the First Transmembrane Domain." *Cell Mol Immunol* 11(2014): 141-149.
13. Schoeman, Dewald, and Burtram C Fielding. "Coronavirus Envelope Protein: Current Knowledge." *Virol J* 16(2019): 1-22.
14. Pilon, Alan C, Marilia Valli, Alessandra C Dametto, and Meri Emili F Pinto, et al. "NuBBE DB: An Updated Database to Uncover Chemical and Biological Information from Brazilian Biodiversity." *Sci Rep* 7(2017): 1-12.
15. Ruch, Travis R, and Carolyn E Machamer "The Coronavirus E Protein: Assembly and Beyond.: *Viruses* 4(2012): 363-382.
16. McBride, Ruth, Marjorie Van Zyl, and Burtram C. Fielding. "The Coronavirus Nucleocapsid is a Multifunctional Protein." *Viruses* 6(2014): 2991-3018.
17. Chang, Chung-ke, Ming-Hon Hou, Chi-Fon Chang, and Chwan-Deng Hsiao, et al. "The SARS Coronavirus Nucleocapsid Protein–Forms and Functions." *Antiviral Res* 103(2014): 39-50.
18. Yan, Renhong, Yuanyuan Zhang, Yaning Li, and Lu Xia, et al. "Structural Basis for the Recognition of SARS-CoV-2 by Full-Length Human ACE2." *Science* 367(2020): 1444-1448.
19. Walls, Alexandra C, Young-Jun Park, M Alejandra Tortorici, and Abigail Wall, et al. "Structure, Function, and Antigenicity of the SARS-CoV-2 Spike Glycoprotein." *Cell* 181(2020): 281-292.
20. Hoffmann, Markus, Hannah Kleine-Weber, Simon Schroeder, and Nadine Krüger, et al. "SARS-CoV-2 Cell Entry Depends on ACE2 and TMPRSS2 and is Blocked by a Clinically Proven Protease Inhibitor." *Cell* 181(2020): 271-280.e8.
21. Kang, Hyojeung, Kanchan Bhardwaj, Yi Li, and Satheesh Palaninathan, et al. "Biochemical and Genetic Analyses of Murine Hepatitis Virus Nsp15 Endoribonuclease." *J Virol* 81(2007): 13587-13597.
22. Bhardwaj, Kanchan, Jingchuan Sun, Andreas Holzenburg, and Linda A Guarino, et al. "RNA Recognition and Cleavage by the SARS Coronavirus Endoribonuclease." *J Mol Biol* 361(2006): 243-256.
23. Zhang, Lianqi, Lei Li, Liming Yan, and Zhenhua Ming, et al. "Structural and Biochemical Characterization of Endoribonuclease Nsp15 Encoded by Middle East Respiratory Syndrome Coronavirus." *J Virol* 92(2018): e00893-e00918.
24. Ton, Anh Tien, Francesco Gentile, Michael Hsing, and Fuqiang Ban, et al. "Rapid Identification of Potential Inhibitors of SARS CoV 2 Main Protease by Deep Docking of 1.3 Billion Compounds." *Mol Inform* 39(2020): e2000028.
25. Waterhouse, Andrew, Martino Bertoni, Stefan Bienert, and Gabriel Studer, et al. "SWISS-MODEL: Homology Modelling of Protein Structures and Complexes." *Nucleic Acids Res* 46(2018): W296-W303.
26. Wishart, David S, Yannick D Feunang, An C Guo, and Elvis J Lo, et al. "DrugBank 5.0: A Major Update to the DrugBank Database for 2018." *Nucleic Acids Res* 46(2018): D1074-D1082.
27. Tchesnokov, Egor P, Joy Y Feng, Danielle P Porter, and Matthias Götte. "Mechanism of Inhibition of Ebola Virus RNA-Dependent RNA Polymerase by Remdesivir." *Viruses* 11(2019): 326.
28. Al-Tawfiq, Jaffar A, Ali H Al-Homoud, and Ziad A Memish. "Remdesivir as a Possible Therapeutic Option for the COVID-19." *Travel Med Infect Dis* 34(2020):101615.
29. Poulin, David, and Jon Yard. "Dynamics of a quantum reference frame." *N J Phys* 9(2007): 156.
30. Skotiniotis, Michael, Borzu Toloui, Ian T Durham, and Barry C Sanders. "Quantum Frameness for C P T Symmetry." *Phys Review Lett* 111(2013): 020504.
31. Rovelli, Carlo. "Quantum Reference Systems." *Class Quantum Gravity* 8(1991): 317.
32. Poulin, David. "Toy Model for a Relational Formulation of Quantum Theory." *Int J Theor Phys* 45(2006): 1189-1215.
33. Girelli, Florian, and David Poulin. "Quantum Reference Frames and Deformed Symmetries." *Phys Rev* 77(2008): 104012.
34. Miyadera, Takayuki, Leon Loveridge, and Paul Busch. "Approximating Relational Observables by Absolute Quantities: A Quantum Accuracy-Size Trade-Off." *J Phys* 49(2016): 185301.
35. Loveridge, Leon, Paul Busch, and Takayuki Miyadera. "Relativity of Quantum States and Observables." *EPL* (Europhys Lett) 117(2017): 40004.
36. Kunduri, HK, and J Lucietti. "Classification of Near-Horizon Geometries of Extremal Black Holes." *Living Rev Relativ* 16(2013): 8.
37. Yoshida, Naoki. "Formation of the First Generation of Stars and Blackholes in the Universe." *Proc Jpn Acad Ser B Phys Biol Sci* 95(2019): 17-28.
38. Bertschinger, Edmund. "Simulations of Structure Formation in the Universe." *Annu Rev Astron Astrophys* 36(1998): 599-654.
39. Birrell, Nicholas David, Nicholas David Birrell, PCW Davies, and Paul Davies. "Quantum Fields in Curved Space." *Cambridge University Press* (1984).

40. Baumgarte, Thomas W, and Stuart L Shapiro. "Numerical Integration of Einstein's Field Equations." *Phys Rev D* 59(1998): 024007.

41. Anninos, Peter, Joan Massó, Edward Seidel, and Wai-Mo Suen, et al. "Dynamics of Gravitational Waves in 3D: Formulations, Methods, and Tests." *Phys Rev D* 56(1997): 842.

42. Anninos, Peter, Joan Centrella, and Richard A. Matzner. "Nonlinear Wave Solutions to the Planar Vacuum Einstein Equations." *Phys Rev D Part Fields* 43(1991): 1825-1838.

43. Anninos, Peter, Joan Centrella, and Richard Matzner. "Nonlinear solutions for initial data in the vacuum Einstein equations in plane symmetry." *Phys Rev D Part Fields* 39(1989): 2155-2171.

44. Chou, Yu-Ching. "A Radiating Kerr Black Hole and Hawking Radiation." *Heliyon* 6(2020): e03336.

How to cite this article: Grigoriadis, Ioannis. "Gallilean Black Hole Transformations for the Anti COVID19 RoccuffirnaTM Drug Design." Clin Schizophr Relat Psychoses Spl 1(2020). DOI: 10.3371/CSRP.GJ.112820.